

Deep Weakly-supervised Anomaly Detection

Guansong Pang · Chunhua Shen · Huidong Jin ·
Anton van den Hengel

Received: date / Accepted: date

Abstract Anomaly detection is typically posited as an unsupervised learning task in the literature due to the prohibitive cost and difficulty to obtain large-scale labeled anomaly data, but this ignores the fact that a limited number (*e.g.*, a few dozens) of labeled anomalies can often be made available with small/trivial cost in many real-world anomaly detection applications. To leverage such labeled anomaly data, we study an important anomaly detection problem termed *weakly-supervised anomaly detection*, in which, in addition to a large amount of unlabeled data, a limited number of labeled anomalies are available during modeling. Learning with the small labeled anomaly data enables *anomaly-informed* modeling, which helps identify anomalies of interest and address the notorious high false positives in unsupervised anomaly detection. However, the problem is especially challenging, since (i) the limited amount of labeled anomaly data often, if not always, cannot cover all types of anomalies and (ii) the unlabeled data is often dominated by normal instances but has anomaly contamination. We address the problem by formulating it as a pairwise relation prediction task. Particularly, our approach defines a two-stream ordinal regression neural network to learn the relation of randomly sampled instance pairs, *i.e.*, whether the instance pair contains two labeled anomalies, one labeled anomaly, or just unlabeled data instances. The resulting model effectively leverages both the labeled and unlabeled data to substantially augment the training data and learn well-generalized representations of normality and abnormality. Comprehensive empirical results on 40 real-world datasets show that our approach (i) significantly outperforms six state-of-the-art methods in detecting both of the known and previously unseen anomalies and (ii) is substantially more data-efficient.

Guansong Pang · Chunhua Shen · Anton van den Hengel
Australian Institute for Machine Learning
University of Adelaide
Adelaide, SA 5005, Australia
E-mail: {guansong.pang, chunhua.shen, anton.vandenhengel}@adelaide.edu.au

Huidong Jin
CSIRO Data61,
Canberra, ACT 2601, Australia
E-mail: warren.jin@csiro.au

1 Introduction

Anomaly detection aims at identifying exceptional data instances that have a significant deviation from the majority of data instances, which can offer important insights into broad applications, such as identifying fraudulent transactions or insider trading, detecting network intrusions, and early detection of diseases or adverse drug reactions. Numerous anomaly detection methods have been introduced (Breunig et al. 2000; Jin et al. 2008; Kriegel et al. 2008; Zhang et al. 2009; Jin et al. 2010; Liu et al. 2012; Chen et al. 2017; Schlegl et al. 2017; Zenati et al. 2018; Pang et al. 2018; Ruff et al. 2018; Pang et al. 2019; Zheng et al. 2019), of which most are unsupervised methods. The popularity of the unsupervised methods is mainly because that they avoid the prohibitive cost associated with labeling large-scale anomaly data, which is required in fully-supervised approaches. However, since they do not have any prior knowledge of the anomalies of interests, many anomalies they identify are often data noises or uninteresting data instances, leading to high false positives or low detection recall. More importantly, although collecting large-scale anomaly data is often too costly (if not impossible), a very small number of labeled anomalies can often be made available with small/trivial cost in many real-world anomaly detection applications. Those labeled anomalies provide strong indication of the anomalies of interests and should be well leveraged to enable more accurate anomaly detection. Those labeled anomaly data may come from a deployed detection system, *e.g.*, a few successfully detected network intrusion records, or they may be from end-users, such as a small number of fraudulent credit card transactions that are reported by bank clients.

To address the above issues, we study a more practical anomaly detection problem, termed *weakly-supervised anomaly detection*, in which a limited number of (partially) labeled anomalies and a large amount of unlabeled data are provided at the training stage. This problem allows us to build anomaly-informed detection models which help identify anomalies of interest and address the notorious high false positive errors in unsupervised anomaly detection (Aggarwal 2017). Furthermore, it requires only a very small amount of labeled anomaly data, eliminating the reliance on large-scale and complete labeled anomaly data in fully-supervised approaches.

However, this problem is especially challenging. This is because we have only limited labeled data for the anomaly class, and moreover, anomalies typically stem from unknown events. Therefore, the limited labeled anomalies often, if not always, cannot cover all types of anomalies. As a result, those limited anomalies can only provide incomplete supervision information, and thus, one significant challenge here is to generalize from those limited incomplete labeled anomaly data to detect *known anomalies* (*i.e.*, anomalies that demonstrate similar abnormal behaviors to the labeled anomalies) and *unknown anomalies* (*i.e.*, new types of anomalies that are unknown during training). Another main challenge lies on the difficulty of leveraging the large unlabeled data that is often dominated by normal instances but has anomaly contamination.

To address the proposed problem, this paper introduces a novel anomaly detection formulation and its instantiation, namely Pairwise Relation prediction-based Ordinal regression Network (PRO). Particularly, the problem is formulated as a *surrogate* supervised learning task, of which a *two-stream ordinal regression neural network* is defined to predict the relation of randomly sampled instance pairs, *i.e.*, to discriminate whether a instance pair contains two labeled anomalies, only one labeled anomaly, or just unlabeled instances. To achieve this goal, PRO first generates pairs of instances sampled from the small labeled anomaly data and the large unlabeled data, and then augments the pairs with a *synthetic ordinal class* feature, in which a large *scalar* value for the instance pairs with two labeled anomalies, and an

intermediate value for the pairs with one labeled anomaly and one unlabeled instance, and a small value for the other pairs with unlabeled instances are assigned. PRO further feeds these pairwise samples into the two-stream regression network to minimize the differences between the regression predictions and the synthetic ordinal labels. The model is therefore optimized to output larger prediction scores for the input pairs that contain two anomalies than the pairs with one anomaly or none. By doing so, the prediction scores can be inherently defined as the anomaly scores of the pairs. In other words, PRO simultaneously optimizes the pairwise relation prediction and anomaly score learning. At the testing/detecting stage, PRO pairs a new instance with the training instances and uses the regression network to infer its anomaly score.

There have been a few early explorations in this research line using traditional methods (McGlohon et al. 2009; Tamersoy et al. 2014; Zhang et al. 2018) or recently emerged deep anomaly detection methods¹ (Pang et al. 2018), but they leverage the labeled anomalies as auxiliary data to enhance an existing anomaly measure or perform a classification-based anomaly detection. This may lead to insufficient exploitation of the labeled data and/or poor generalization. Our very recent work (Pang et al. 2019) is the most relevant work, in which a method called deviation network (DevNet) is introduced to leverage the few labeled anomalies and unlabeled data to learn representations of both normality and abnormality. It is done by enforcing the anomaly scores of individual data instances to fit a one-sided Gaussian distribution, achieving significant improvement over current state-of-the-arts. PRO is motivated by the success of DevNet, but they represent two completely different approaches. DevNet leverages the Gaussian prior to learn the anomaly scores and it may fail to work when the prior is inexact, whereas PRO learns the anomaly scores by ordinal regression and does not involve any probability distribution assumption over the anomaly scores, enabling PRO to learn more faithful representations than DevNet. Furthermore, the pairwise relation prediction substantially augments the labeled data and enables PRO to learn more diverse representations of normality and abnormality other than that in DevNet, resulting in substantially better generalization ability.

Additionally, note that well established semi-supervised anomaly detection (Noto et al. 2012; Ienco et al. 2017; Aggarwal 2017) focuses on learning patterns of the normal class using *large labeled normal data*. By contrast, the weakly-supervised setting here is to take full advantage of *limited (often incomplete) labeled anomaly data* to learn detection models that are highly generalized to detect both the known and unknown anomalies. As a result, these two problems are different in terms of the given data and the nature of the problem. These differences are summarized in Table 1. On the other hand, the term ‘weakly-supervised’ is also intentionally used to emphasize the nature of the incompleteness of the labeled data in our setting (Zhou 2018).

Table 1 Weakly- and Semi-supervised Anomaly Detection Settings

Approach	Training Data	Problem
Semi-supervised	Large <i>labeled normal data</i> and unlabeled data	Learn patterns of labeled normal data
Weakly-supervised	<i>Limited (partially) labeled anomaly data</i> , large unlabeled data	Learn to generalize from a few labeled known anomalies to detect both known and unknown anomalies

¹ Deep anomaly detection methods refer to any methods that exploit deep learning techniques (Goodfellow et al. 2016) to learn feature representations or anomaly scores for anomaly detection.

In summary, this work makes the following four main contributions.

- We propose a novel formulation for synthesizing pairing-based data augmentation and ordinal regression to achieve deep weakly-supervised anomaly detection via pairwise relation learning. This approach substantially augments the labeled data and learns *anomaly-informed* detection models with desired *generalizability*.
- A novel method, namely PRO, is instantiated from our formulation to simultaneously learn the pairwise relations and anomaly scores by training a two-stream ordinal regression neural network, achieving *data-efficient* learning and well-generalized models to detect known and unknown anomalies.
- We theoretically and empirically show that our two-stream ordinal regression network can effectively leverage the large unlabeled data while being tolerant to small anomaly contamination.
- As a result, we show by our empirical results on 40 real-world datasets, including 12 datasets that contain known anomalies and 28 datasets that contain exclusively unknown anomalies, that PRO (i) significantly outperforms four state-of-the-art competing methods in detecting both known and unknown anomalies, *e.g.*, achieving 10%-30% improvement in precision-recall rates in detecting unknown anomalies, and (ii) obtains a substantially better data efficiency, *e.g.*, it requires 50%-87.5% less labeled anomalies to perform comparably well to, or substantially better than, the best contenders.

2 Learning Anomaly Scores by Predicting Pairwise Relation

2.1 Problem Formulation

Given a training dataset $\mathcal{X} = \{\mathbf{x}_1, \mathbf{x}_2, \dots, \mathbf{x}_N, \mathbf{x}_{N+1}, \dots, \mathbf{x}_{N+K}\}$ of size $N + K$, with $\mathbf{x}_i \in \mathbb{R}^D$, where $\mathcal{U} = \{\mathbf{x}_1, \mathbf{x}_2, \dots, \mathbf{x}_N\}$ is a large unlabeled dataset and $\mathcal{A} = \{\mathbf{x}_{N+1}, \mathbf{x}_{N+2}, \dots, \mathbf{x}_{N+K}\}$ with $K \ll N$ is a very small set of labeled anomalies that provide some prior knowledge of anomalies, our goal is to learn an anomaly scoring function $\phi : \mathcal{X} \mapsto \mathbb{R}$ that assigns anomaly scores to data instances in a way that we have $\phi(\mathbf{x}_i) > \phi(\mathbf{x}_j)$ if \mathbf{x}_i is an anomaly and \mathbf{x}_j is a normal data instance.

To obtain more labeled data and effectively leverage both the small labeled anomalies and large unlabeled data, we formulate the problem as a pairwise relation learning task, of which we learn to discriminate three types of *unordered* random instance pairs, including anomaly-anomaly pair, anomaly-unlabeled pair, unlabeled-unlabeled pair. More importantly, since our primary goal is to learn anomaly scores, we aim to unify the relation learning and anomaly scoring such that the learner assigns substantially larger anomaly scores to the data instance pairs that contain anomalies than the other instance pairs. This can be achieved by formulating the relation learning task as an ordinal regression task. Specifically, let $\mathcal{P} = \{(\mathbf{x}_i, \mathbf{x}_j, y_{\{\mathbf{x}_i, \mathbf{x}_j\}}) \mid \mathbf{x}_i, \mathbf{x}_j \in \mathcal{X} \text{ and } y_{\{\mathbf{x}_i, \mathbf{x}_j\}} \in \mathbb{N}\}$ be a set of pairs of randomly sampled instances with artificial class labels, where each pair $\{\mathbf{x}_i, \mathbf{x}_j\}$ has one of the three pairwise relations: $C_{\{\mathbf{a}, \mathbf{a}\}}$, $C_{\{\mathbf{a}, \mathbf{u}\}}$ and $C_{\{\mathbf{u}, \mathbf{u}\}}$ ($\mathbf{a} \in \mathcal{A}$ and $\mathbf{u} \in \mathcal{U}$) and $\mathbf{y} \in \mathbb{N}^{|\mathcal{P}|}$ is an ordinal class feature with *decreasing* value assignments to the respective $C_{\{\mathbf{a}, \mathbf{a}\}}$, $C_{\{\mathbf{a}, \mathbf{u}\}}$ and $C_{\{\mathbf{u}, \mathbf{u}\}}$ pairs, *i.e.*, $y_{\{\mathbf{a}, \mathbf{a}\}} > y_{\{\mathbf{a}, \mathbf{u}\}} > y_{\{\mathbf{u}, \mathbf{u}\}}$, then the pairwise relations and anomaly scores are simultaneously learned by training a *ternary* ordinal regression function $\phi : \mathcal{P} \mapsto \mathbb{R}$.

2.2 The Instantiated Model: PRO

Our deep anomaly detection method PRO is then instantiated from the formulation, which simultaneously learns pairwise relations and anomaly scores by training an end-to-end ordinal regression neural network. As shown in Fig. 1, PRO consists of three modules: pairing data augmentation, end-to-end anomaly score learner and ordinal regression. The data augmentation generates the instance pair set \mathcal{P} . The relation learning (anomaly scoring) function ϕ is a composition of a feature learner ψ and a relation (anomaly score) learner η , which can be trained in an end-to-end manner with an ordinal regression loss function.

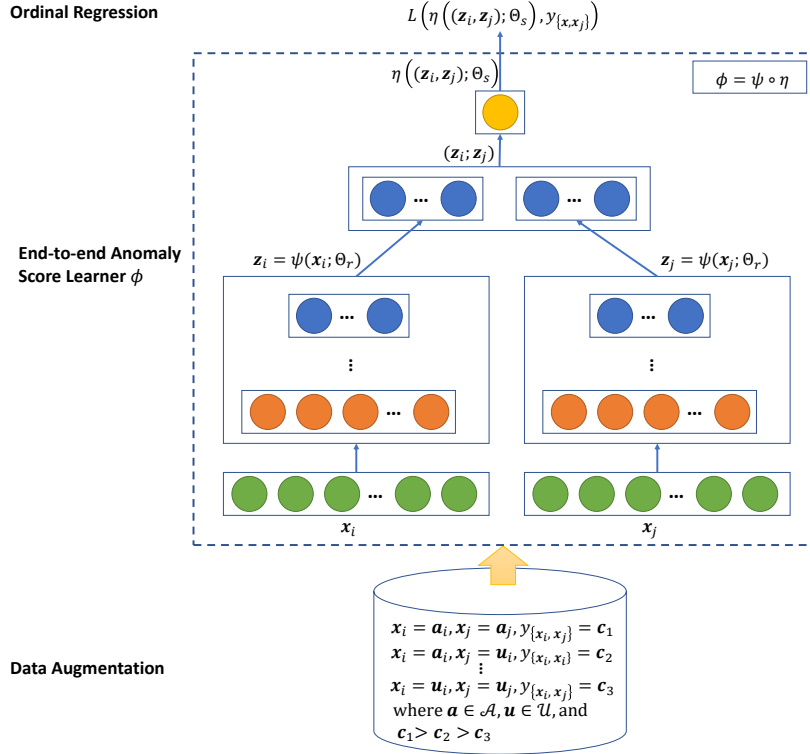


Fig. 1 PRO - Pairwise Relation prediction-based ordinal regression Network. It takes $C_{\{a,a\}}$, $C_{\{a,u\}}$ and $C_{\{u,u\}}$ instance pairs as inputs and learns to discriminate the three types of pairwise relations while at the same time yielding *decreasing* prediction scores to the respective $C_{\{a,a\}}$, $C_{\{a,u\}}$ and $C_{\{u,u\}}$ instance pairs. These prediction scores are inherently coupled with the discrimination of anomalies and normal instances and thus can be used as anomaly scores.

2.2.1 Data Augmentation by Pairing

Different from popular editing-based augmentation (Zhang and LeCun 2015; Perez and Wang 2017), a two-step pairing-based data augmentation method is used for our problem to substantially extend the labeled data: (i) we first generate a set of instance pairs with instances randomly sampled from the small labeled anomaly set \mathcal{A} and the large unlabeled

dataset \mathcal{U} , and categorize the pairs into three classes $C_{\{\mathbf{a}, \mathbf{a}\}}$, $C_{\{\mathbf{a}, \mathbf{u}\}}$ and $C_{\{\mathbf{u}, \mathbf{u}\}}$ based on the sources that the instances of each pair sample from, where $\mathbf{a} \in \mathcal{A}$ and $\mathbf{u} \in \mathcal{U}$; and (ii) a synthetic ordinal class feature \mathbf{y} is then added, in which the instance pairs of the three classes are assigned with *scalar* class labels, such that $y_{\{\mathbf{a}, \mathbf{a}\}} = c_1$, $y_{\{\mathbf{a}, \mathbf{u}\}} = c_2$, $y_{\{\mathbf{u}, \mathbf{u}\}} = c_3$ and $c_1 > c_2 > c_3 \geq 0$. By doing so, we efficiently synthesize \mathcal{A} and \mathcal{U} to produce a large fully labeled dataset $\mathcal{P} = \{(\mathbf{x}_i, \mathbf{x}_j, y_{\{\mathbf{x}_i, \mathbf{x}_j\}}) \mid \mathbf{x}_i, \mathbf{x}_j \in \mathcal{X} \text{ and } y_{\{\mathbf{x}_i, \mathbf{x}_j\}} \in \mathbb{N}\}$.

More importantly, \mathcal{P} contains critical information for discriminating anomalies from normal data instances. This is due to the fact that, as anomalies are rare data instances, the unlabeled dataset \mathcal{U} is often dominated by normal data instances. As a result, most $C_{\{\mathbf{u}, \mathbf{u}\}}$ pairs consist of normal instances only. Thus, with \mathcal{P} as data inputs, PRO is fed with training samples that contain key information for discriminating anomalies and normal instances, since $C_{\{\mathbf{a}, \mathbf{a}\}}$, $C_{\{\mathbf{a}, \mathbf{u}\}}$ and $C_{\{\mathbf{u}, \mathbf{u}\}}$ are approximately anomaly-anomaly, anomaly-normal and normal-normal pairs. Note that a few $C_{\{\mathbf{a}, \mathbf{u}\}}$ and $C_{\{\mathbf{u}, \mathbf{u}\}}$ pairs may contain some noisy pairs from this aspect due to potential anomaly contamination in \mathcal{U} , but we found theoretically and empirically that PRO is generally robust to these noisy pairs (see Sections 3.2 and 4.7.1 for detail).

2.2.2 End-to-end Anomaly Score Learner

An end-to-end anomaly score (or pairwise relation) learner is then defined to take pairs of data instances as inputs and directly output the anomaly scores of the pairs. Let $\mathcal{Z} \in \mathbb{R}^M$ be an intermediate representation space, we define a two-stream anomaly scoring network $\phi((\cdot, \cdot); \Theta) : \mathcal{P} \mapsto \mathbb{R}$ as a composition of a feature learner $\psi(\cdot; \Theta_r) : \mathcal{X} \mapsto \mathcal{Z}$ and an anomaly scoring function $\eta((\cdot, \cdot); \Theta_s) : (\mathcal{Z}, \mathcal{Z}) \mapsto \mathbb{R}$, where $\Theta = \{\Theta_r, \Theta_s\}$. Specifically, $\psi(\cdot; \Theta_r)$ is a neural *feature learner* with $H \in \mathbb{N}$ hidden layers and weight matrices $\Theta_r = \{\mathbf{W}^1, \mathbf{W}^2, \dots, \mathbf{W}^H\}$:

$$\mathbf{z} = \psi(\mathbf{x}; \Theta_r), \quad (1)$$

where $\mathbf{x} \in \mathcal{X}$ and $\mathbf{z} \in \mathcal{Z}$. Different network structures can be used here, such as multilayer perceptrons for multidimensional data, convolutional networks for image data, or recurrent networks for sequence data (Goodfellow et al. 2016).

$\eta((\cdot, \cdot); \Theta_s)$ is defined as an *anomaly score learner* which uses a linear neural unit in the output layer to compute the anomaly scores based on the intermediate representations:

$$\eta((\mathbf{z}_i, \mathbf{z}_j); \Theta_s) = \sum_{k=1}^M w_k^o z_{ik} + \sum_{l=1}^M w_{M+l}^o z_{jl} + w_{2M+1}^o, \quad (2)$$

where $\mathbf{z} \in \mathcal{Z}$, $(\mathbf{z}_i, \mathbf{z}_j)$ is a *concatenation* operation of \mathbf{z}_i and \mathbf{z}_j , and $\Theta_s = \{\mathbf{w}^o\}$, in which $\{w_1^o, w_2^o, \dots, w_{2M}^o\}$ are weight parameters and w_{2M+1}^o is a bias term. As shown in Fig. 1, to reduce the optimization complexity, PRO uses a two-stream network with the shared weight parameters Θ_r to learn the representations \mathbf{z}_i and \mathbf{z}_j .

Lastly $\phi((\cdot, \cdot); \Theta)$ can be formally represented as

$$\phi((\mathbf{x}_i, \mathbf{x}_j); \Theta) = \eta((\psi(\mathbf{x}_i; \Theta_r), \psi(\mathbf{x}_j; \Theta_r)); \Theta_s), \quad (3)$$

which can be trained in an end-to-end fashion to directly map data inputs to scalar scores.

Note that the concatenation results in an *ordered* pair $(\mathbf{z}_i, \mathbf{z}_j)$. This does not affect the unordered pairs from the $C_{\{\mathbf{a}, \mathbf{a}\}}$ and $C_{\{\mathbf{u}, \mathbf{u}\}}$ classes since the instances of these pairs come from the same dataset (*i.e.*, \mathcal{A} or \mathcal{U}), but it may produce inverse effects on our training with

the $C_{\{a,u\}}$ pairs. This problem is addressed by organizing all unordered $C_{\{a,u\}}$ and $C_{\{u,a\}}$ pairs into consistently the same type of ordered pairs, *e.g.*, $C_{(a,u)}$, before training, which will reduce one unnecessarily model parameter in ordinal regression below.

2.2.3 Ordinal Regression

PRO then feeds the ordinal class labels and the anomaly scores yielded by ϕ to optimize the scores using an ordinal regression objective, *i.e.*, minimizing the difference between the prediction scores and the ordinal labels $y_{\{a,a\}}$, $y_{\{a,u\}}$ and $y_{\{u,u\}}$. It is equivalent to assigning larger prediction scores to the $C_{\{a,a\}}$ and $C_{\{a,u\}}$ instance pairs than the $C_{\{u,u\}}$ instance pairs. Our loss is defined as below to guide the optimization:

$$L\left(\phi((\mathbf{x}_i, \mathbf{x}_j); \Theta), y_{\{\mathbf{x}_i, \mathbf{x}_j\}}\right) = \left| y_{\{\mathbf{x}_i, \mathbf{x}_j\}} - \phi((\mathbf{x}_i, \mathbf{x}_j); \Theta) \right|. \quad (4)$$

The absolute prediction error, instead of square error, is used in the loss to reduce the effect of potential noisy pairs due to the anomaly contamination in \mathcal{U} . The three class labels $y_{\{a,a\}} = 8$, $y_{\{a,u\}} = 4$ and $y_{\{u,u\}} = 0$ are used by default to enforce large margins among the anomaly scores of the three types of instance pairs. PRO also works very well with other value assignments as long as there are reasonably large margins among the ordinal class labels. Therefore, the overall objective function can be written as

$$\arg \min_{\Theta} \frac{1}{|\mathcal{B}|} \sum_{(\mathbf{x}_i, \mathbf{x}_j, y_{\{\mathbf{x}_i, \mathbf{x}_j\}}) \in \mathcal{B}} \left| y_{\{\mathbf{x}_i, \mathbf{x}_j\}} - \phi((\mathbf{x}_i, \mathbf{x}_j); \Theta) \right| + \lambda R(\Theta), \quad (5)$$

where \mathcal{B} is a sample batch from \mathcal{P} and $R(\Theta)$ is a regularization term with the hyperparameter λ . The detailed optimization settings are provided in Section 4.2.

2.3 Anomaly Detection Using PRO

2.3.1 Training Stage

Algorithm 1 presents the procedure of training PRO. Step 1 first extends the data \mathcal{X} into a set of instance pairs with ordinal class labels, \mathcal{P} . After an uniform *Glorot* weight initialization (Glorot and Bengio 2010) in Step 2, PRO performs stochastic gradient descent (SGD) based optimization to learn Θ in Steps 3-9 and obtains the optimized ϕ in Step 10. Particularly, stratified random sampling is used in Step 5 to ensure the sample balance of the three classes in \mathcal{B} , *i.e.*, for each batch $\frac{|\mathcal{B}|}{2}$ instance pairs are sampled from the $C_{\{u,u\}}$ class and $\frac{|\mathcal{B}|}{4}$ instance pairs are respectively sampled from the $C_{\{a,a\}}$ and $C_{\{a,u\}}$ classes. This is equivalent to oversampling the two anomaly-related classes, $C_{\{a,a\}}$ and $C_{\{a,u\}}$, to avoid bias towards the $C_{\{u,u\}}$ class due to the class-imbalance problem. Step 6 performs the forward propagation of the network and computes the loss. Step 7 then uses the loss to perform gradient descent steps.

Algorithm 1 *Training PRO*

Input: $\mathcal{X} \in \mathbb{R}^D$ with $\mathcal{X} = \mathcal{U} \cup \mathcal{A}$ and $\emptyset = \mathcal{U} \cap \mathcal{A}$
Output: $\phi : (\mathcal{X}, \mathcal{X}) \mapsto \mathbb{R}$ - an anomaly score mapping

- 1: $\mathcal{P} \leftarrow$ Augment the training data with \mathcal{U} and \mathcal{A}
- 2: Randomly initialize Θ
- 3: **for** $i = 1$ to n_epochs **do**
- 4: **for** $j = 1$ to $n_batches$ **do**
- 5: $\mathcal{B} \leftarrow$ Randomly sample b data instance pairs from \mathcal{P}
- 6: $loss \leftarrow \frac{1}{b} \sum_{(\mathbf{x}_i, \mathbf{x}_j, y_{\{\mathbf{x}_i, \mathbf{x}_j\}}) \in \mathcal{B}} \left| y_{\{\mathbf{x}_i, \mathbf{x}_j\}} - \phi((\mathbf{x}_i, \mathbf{x}_j); \Theta) \right| + \lambda R(\Theta)$
- 7: Perform a gradient descent step w.r.t. the parameters in Θ
- 8: **end for**
- 9: **end for**
- 10: **return** ϕ

2.3.2 Anomaly Scoring Stage

At the testing stage, given a test instance \mathbf{x}_k , PRO first pairs it with data instances randomly sampled from \mathcal{A} and \mathcal{U} , and then defines its anomaly score as

$$s_{\mathbf{x}_k} = \frac{1}{2E} \left[\sum_{i=1}^E \phi((\mathbf{a}_i, \mathbf{x}_k); \Theta^*) + \sum_{j=1}^E \phi((\mathbf{x}_k, \mathbf{u}_j); \Theta^*) \right], \quad (6)$$

where Θ^* are the parameters of a trained ϕ , and \mathbf{a}_i and \mathbf{u}_j are randomly sampled from the respective \mathcal{A} and \mathcal{U} . $s_{\mathbf{x}_k}$ can be interpreted as an ensemble of the anomaly scores of a set of \mathbf{x}_k -oriented pairs. Due to the loss in Eqn. (4), $s_{\mathbf{x}_k}$ is optimized to be greater than $s_{\mathbf{x}'_k}$ given \mathbf{x}_k is an anomaly and \mathbf{x}'_k is a normal instance. The ensemble scores are employed to achieve stable anomaly scoring. PRO can perform very stably as long as the ensemble size E is sufficiently large due to the law of large numbers ($E = 30$ is used by default).

3 Theoretical Foundation of PRO

The performance of the proposed weakly-supervised learning framework and the PRO algorithm are based on two reasonable assumptions. The first one is that the labeled anomalies are correctly labeled, i.e., true anomalies. The second one is that the proportion of true anomalies in the unlabeled data instances is relatively small. The performance of PRO may drop on data sets where neither assumptions is held.

3.1 Transformative Data Augmentation

The underlying purpose of our data augmentation is to leverage both the limited labeled anomaly data and large unlabeled data by transferring a highly imbalanced weakly-supervised anomaly detection problem to a large balanced supervised learning of pairwise relations. First, due to the random sampling of pairwise relations used in PRO, the sample size of the training data theoretically increases from $N + K$ for the weakly-supervised anomaly detection problem to $K^3 N^3$ for the pairwise relation learning, which enables deep learning even for an anomaly detection problem with only a few thousands of unlabeled instances and dozens of labeled anomalies. We have K^2 of $C_{\{\mathbf{a}, \mathbf{a}\}}$ pairwise relations, $K \times N$ of

$C_{\{a,u\}}$ and N^2 of $C_{\{u,u\}}$ relations; in Step 5 of PRO in Algorithm 1, we independently sample from three different pairwise relations, and thus, there are $K^3 N^3$ pairwise relations to choose from. Such a large size clearly helps build up the generalizability and then the detection performance of our anomaly detection model. Note that PRO uses a shared-weight two-stream network in its representation learner $\psi(\cdot; \Theta_r)$, so the representation learning is still optimized on the original \mathcal{X} data space rather than the pairwise higher-order \mathcal{P} space. This trick well supports the scale-up of the training sample size while adding nearly no extra model complexity.

Furthermore, in Step 5 of PRO, we sample about a quarter of pairwise relations from $C_{\{a,a\}}$, a quarter from $C_{\{a,u\}}$, and half from $C_{\{u,u\}}$. That means, about half of data instances in these pairwise relations are from labeled anomalies. Through oversampling pairwise relations from $C_{\{a,a\}}$ and $C_{\{a,u\}}$, labeled anomalies are relatively balanced with unlabeled data instances, during the ‘supervised’ anomaly score learning in Steps 5 and 6. Thus, the imbalance issue caused by $K \ll N$, which often substantially deteriorates learning performance, is massaged.

More importantly, the pairwise interaction between the pair samples of $C_{\{a,a\}}$ or $C_{\{a,u\}}$ carries diverse information from each other, and the corresponding pairwise data space is significantly larger than that of the small labeled anomaly set \mathcal{A} . Thus, oversampling from these two pairwise sample pools substantially augments our training data with naturally diverse and discriminative pairwise anomaly-related samples, providing substantially richer anomaly supervision information than oversampling from the small anomaly set \mathcal{A} only.

This augmented data enables significantly improved generalizability in detecting both known and unknown anomalies. Additionally, the ternary ordinal regression enables PRO to learn the representations of respective anomaly-anomaly, anomaly-normal and normal-normal interactions; and Eqn. (6) considers every two possible combination of these three types of representations to infer anomaly scores. That means PRO performs anomaly scoring using a collective energy of two-level hierarchical representations, *i.e.*, representations of $C_{\{a,a\}}$, $C_{\{a,u\}}$ and $C_{\{u,u\}}$ and their pairwise combinations. This enables PRO to spot the abnormality from multiple different aspects. PRO can therefore identify subtle or unknown anomalies when their pairwise interaction with training instances demonstrate similar patterns to the anomaly-anomaly/normal relations, or deviated patterns from the anomaly/normal-normal relations.

3.2 End-to-end Anomaly Score Optimization with Ordinal Regression

We assume the proportion of true anomalies in the unlabeled data instances, ϵ , is small, say $\leq 5\%$, which is normally the case in real-world applications (Aggarwal 2017). Based on randomly sampling, we can obtain the expectation of the pairwise relation proportions in each batch \mathcal{B} in Step 5 of PRO in Algorithm 1. Specifically, there are $\frac{1}{4} + \frac{1}{4}\epsilon + \frac{1}{2}\epsilon^2$ from true anomaly-anomaly pairwise relations, and $\frac{1}{4} + \frac{3}{4}\epsilon - \epsilon^2$ from true anomaly-normal pairwise relations, and $\frac{1}{2} - \epsilon + \frac{1}{2}\epsilon^2$ from normal-normal pairwise relations. Thus, a small percentage of the pairwise relations, $2\epsilon - \epsilon^2$, could have mis-assigned ordinal labels during the data augmentation procedure. Considering the tolerance of the regression performance to these outliers (She and Owen 2011; Yu and Yao 2017), PRO can perform well when the proportion of true anomalies in the unlabeled data instances is reasonably small, say $\leq 5\%$. With the recent development of regression techniques (Yu and Yao 2017), the breakdown point of modern robust regression techniques could reach as large as 50%, *e.g.*, through reaching a nice tradeoff iteratively between the regularization term and the loss term (She and Owen

2011). Breakdown point is to measure the proportion of anomalies that a regression estimate can tolerate before it goes to infinity. That means the proposed technique may have potential to tolerate ϵ around 25%. We will leave realizing the full potential to future work, though our experimental results in Section 4.7.1 will illustrate the reliable performance of the proposed PRO to different level of noises in the unlabeled data.

On the other hand, from the regression modeling, we have expectation for different type of pairwise relations for true anomaly \mathbf{a}_k and normal data instance \mathbf{n}_l :

$$\begin{aligned}\mathbb{E}[\phi((\mathbf{a}_i, \mathbf{a}_k); \Theta^*)] &= c_1, \\ \mathbb{E}[\phi((\mathbf{a}_k, \mathbf{u}_j); \Theta^*)] &= c_2, \\ \mathbb{E}[\phi((\mathbf{a}_i, \mathbf{n}_l); \Theta^*)] &= \mathbb{E}[\phi((\mathbf{a}_i, \mathbf{u}_j); \Theta^*)] - \epsilon \mathbb{E}[\phi((\mathbf{a}_i, \mathbf{a}_j); \Theta^*)] \\ &= c_2 - \epsilon c_1, \\ \mathbb{E}[\phi((\mathbf{n}_l, \mathbf{u}_j); \Theta^*)] &= \mathbb{E}[\phi((\mathbf{u}_i, \mathbf{u}_j); \Theta^*)] - \epsilon \mathbb{E}[\phi((\mathbf{a}_i, \mathbf{u}_j); \Theta^*)] \\ &= c_3 - \epsilon c_1.\end{aligned}$$

Thus, from Eqn. (6), we have

$$\begin{aligned}\mathbb{E}[s_{\mathbf{x}_k} | \mathbf{x}_k \text{ is an anomaly}] &= \frac{1}{2E} \left\{ E \times \mathbb{E}[\phi((\mathbf{a}_i, \mathbf{a}_k); \Theta^*)] \right. \\ &\quad \left. + E \times \mathbb{E}[\phi((\mathbf{a}_k, \mathbf{u}_j); \Theta^*)] \right\} = \frac{c_1 + c_2}{2}, \quad (7)\end{aligned}$$

and

$$\begin{aligned}\mathbb{E}[s_{\mathbf{x}_k} | \mathbf{x}_k \text{ is normal}] &= \frac{1}{2E} \left\{ E \times \mathbb{E}[\phi((\mathbf{a}_i, \mathbf{n}_l); \Theta^*)] \right. \\ &\quad \left. + E \times \mathbb{E}[\phi((\mathbf{n}_l, \mathbf{u}_j); \Theta^*)] \right\} = \frac{c_2 + c_3 - 2\epsilon c_1}{2}. \quad (8)\end{aligned}$$

As $c_1 > c_2 > c_3 \geq 0$, $\frac{c_1 + c_2}{2} > \frac{c_2 + c_3 - 2\epsilon c_1}{2}$ for small ϵ . That means PRO is optimized in an end-to-end fashion to guarantee that a true anomaly is expected to have a larger anomaly score than normal instances when the anomaly contamination in the unlabeled data is small.

There have been theoretical analyses for sampling from imbalanced data in anomaly detection. Most of them are for distance-based anomaly measures and/or unsupervised learning (Wu and Jermaine 2006; Sugiyama and Borgwardt 2013; Aggarwal and Sathe 2015), whereas our analysis above is for deep ordinal regression-based measures under the weakly-supervised setting. For example, for domains where distance computation is very expensive, Wu and Jermaine (2006) proposed a sampling-based approach to efficiently approximate the k th-nearest-neighbor distance score, where a subset of data is randomly and iteratively sampled for each instance. To guarantee its detection accuracy, they gave two efficient methods and theoretical analyses of anomaly detection accuracy expectation and variance for its sampling scheme under some reasonable distribution assumption. Sugiyama and Borgwardt (2013) gave a very simple distance-based anomaly detection technique that defines anomalousness of a data instance as its minimum distance to a given random subset of data. Sugiyama and Borgwardt (2013) further theoretically proved that this simple anomaly measure is guaranteed to work well with a small random subset under the assumption that normal instances can be well partitioned into clusters and the random subset contains at least one instance sampled from each of these clusters. Aggarwal and Sathe (2015) gave

a bias-variance tradeoff theory for anomaly detection ensembles by assuming there is an oracle. The theory is almost identical to that in classification. To reduce variance after ensembling, via improving independence and diversity among component methods, Aggarwal and Sathe (2015) proposed two promising ensembling methods, variable subsampling and rotated bagging.

4 Experiments

We aim to empirically examine the following five questions:

- **Detection of both known and unknown anomalies.** Can PRO generalize from a limited number of labeled anomalies to effectively detect both the known and unknown anomalies in real-world datasets?
- **Effectiveness of leveraging the limited labeled data.** How effective is PRO in learning detection models with different amount of labeled data?
- **Tolerance to Anomaly Contamination.** How tolerant is PRO to the anomaly contamination in the unlabeled data?
- **Importance of each individual component of PRO.** How does each individual component of PRO contribute to the overall performance of PRO?
- **Sensitivity of PRO.** Can PRO work stably under different settings of its hyperparameters?

4.1 Datasets

To explicitly evaluate the performance of detecting known and unknown anomalies, we separate our datasets into two groups, including one group contains 12 datasets used for detection of known anomalies and another group contains 28 datasets designed to exclusively evaluate the performance of detecting unknown anomalies.

As shown in Table 2, 12 widely-used publicly available real-world datasets² are used for detection of known anomalies, which are from diverse domains, *e.g.*, intrusion detection, fraud detection, and disease detection (Moustafa and Slay 2015; Liu et al. 2012; Pang et al. 2019). Specifically, the *donors* data is taken from KDD Cup 2014 for predicting excitement of donation projects, with exceptionally exciting projects used as anomalies (6.0% of all data instances). The *census* data is extracted from the US census bureau database, in which we aim to detect the rare high-income persons (6.0%). *fraud* is for fraudulent credit card transaction detection, with fraudulent transactions (0.2%) as anomalies. *celeba* contains more than 200K celebrity images, each with 40 attribute annotations. We use the *bald* attribute as our detection target, in which the scarce *bald* celebrities (3.0%) are treated as anomalies and the other 39 attributes form the feature space. The *dos*, *rec*, *fuz* and *bac* datasets are derived from a popular intrusion detection dataset called *UNSW-NB15* (Moustafa and Slay 2015) with the respective DoS (15.0%), reconnaissance (13.1%), fuzzers (3.1%) and backdoor (2.4%) attacks as anomalies against the ‘normal’ class. *w7a* is a web page classification dataset, with

² *donors* and *fraud* are publicly available at <https://www.kaggle.com/>, *w7a* and *news20* are available at <https://www.csie.ntu.edu.tw/~cjlin/libsvmtools/datasets/>, *dos*, *rec*, *fuz*, *bac* are available at <https://www.unsw.adfa.edu.au/unsw-canberra-cyber/cybersecurity/ADFA-NB15-Datasets/>, *celeba* is at <http://mmlab.ie.cuhk.edu.hk/projects/CelebA.html>, and the other datasets are accessible at <https://archive.ics.uci.edu/ml/datasets/>.

the minority classes (3.0%) as anomalies. *campaign* is a dataset of bank marketing campaigns, with rarely successful campaigning records (11.3%) as anomalies. *news20* is one of the most popular text classification corpora, which is converted into anomaly detection data via random downsampling of the minority class (5.0%) based on (Liu et al. 2012; Zimek et al. 2013). *thyroid* is for disease detection, in which the anomalies are the hypothyroid patients (7.4%). Seven of these datasets contain real anomalies, including *donors*, *fraud*, *dos*, *rec*, *fuz*, *bac* and *thyroid*. The other five datasets contain semantically real anomalies, *i.e.*, they are rare and very different from the majority of data instances. So, they serve as a good testbed for the evaluation of anomaly detection techniques.

To replicate the real-world scenarios where we have a few labeled anomalies and large unlabeled data, we first have a stratified split of the anomalies and normal instances into two subsets, with 80% data as training data and the other 20% data as holdup test set. Since the unlabeled data is often anomaly-contaminated, we then combine some randomly selected anomalies with the whole normal training data instances to form the unlabeled dataset \mathcal{U} . We further randomly sample a limited number of anomalies from the anomaly class to form the labeled anomaly set \mathcal{A} .

Table 3 presents the 28 datasets for the evaluation of detecting unknown anomalies. These datasets are derived from the above four intrusion attack datasets *dos*, *rec*, *fuz* and *bac*, with data instances spanned by the same feature space. To guarantee that the evaluation data contains unknown anomalies only, the anomaly class in one of these four datasets is held up for evaluation, while the anomalies in any combinations of the remaining three datasets are combined to form the pool of known anomalies. The type of the holdup anomalies is always different from that in the anomaly pool and can be safely treated as unknown anomalies. We have 28 possible permutations under this setting, resulting in 28 datasets with different known and/or unknown anomalies. For the training, \mathcal{A} contains the anomalies sampled from the known anomalies pool, while the evaluation data is composed of the holdup unknown anomaly class and the 20% holdup normal instances.

4.2 Competing Methods and Parameter Settings

PRO is compared with the following state-of-the-art methods from diverse related areas:

- DevNet (Pang et al. 2019). DevNet (deviation network) is a deep weakly-supervised anomaly detection method that uses a Gaussian prior to directly learn the anomaly scores.
- DSVDD (Ruff et al. 2018). DSVDD (deep support vector data description) performs support vector data description-based one-class classification with neural networks. The original DSVDD is unsupervised and cannot make use of the labeled anomalies. We adapted it based on (Tax and Duin 2004) to enforce a large margin between the one-class center and the labeled anomalies while minimizing the center-oriented hypersphere. This adaption enhances DSVDD by over 30% accuracy.
- FSNet (Snell et al. 2017). Prototypical network is a well-known few-shot classification method (denoted as FSNet here), which learns prototypical representations of each class and perform classification based on the distance to the prototypes. We adapt it to our problem by learning respective prototypical representations of the labeled anomalies and the unlabeled data.
- cFSNet. To better handle the class imbalance problem, a cost-sensitive learning classifier, cFSNet, is chosen, which is a variant of FSNet by incorporating a cost matrix into the few-shot prototype-based classification. Since the optimal cost matrix can vary

substantially for different datasets (He and Garcia 2009; Fernández et al. 2018), a grid search of the associated cost is used to address this issue. Particularly, the cost rate $r = cost_a / cost_n$ is searched in a wide range $r = \{1, 2, 4, 8, 16, 32, 64, 128\}$, where $cost_a$ represents the cost of misclassifying anomalies as normal instances and $cost_n$ is the cost of misclassifying normal instances as anomalies; and the best detection performance is reported.

- BPR (Rendle et al. 2009). BPR (Bayesian personalized ranking) is a popular method for the optimization of personalized item ranking (or AUC optimization per user) in recommender systems. It is adapted to optimize anomaly ranking to guarantee that the few labeled anomalies are ranked higher than the unlabeled instances.
- iForest (Liu et al. 2012). iForest is a state-of-the-art unsupervised anomaly detection method that calculates the anomaly scores based on how many steps are required to isolate the data points by random half-space partition.

Since our experiments focus on unordered multidimensional data, multilayer perceptron networks are used. Similar to our findings in (Pang et al. 2018, 2019), we empirically found that all deep methods using an architecture with one hidden layer perform better and more stably than using two or more hidden layers. This may be due to the limit of the available labeled data. Following DevNet, one hidden layer with 20 neural units is used in all deep methods. The ReLU activation function $g(a) = \max(0, a)$ is used. An ℓ_2 -norm regularizer with the hyperparameter setting $\lambda = 0.01$ is applied to avoid overfitting. The RMSprop optimizer with the learning rate 0.001 is used. All deep detectors are trained using 50 epochs, with 20 batches per epoch. The batch size is probed in $\{8, 16, 32, 64, 128, 256, 512\}$. The best fits, 512 in PRO, DevNet and DSVDD, 256 in FSNet, are used by default. cFSNet uses the same settings as FSNet. Oversampling is applied to the labeled anomaly set \mathcal{A} to well train the deep detection models of DevNet, DSVDD, FSNet and cFSNet. Hinge loss function together with k -nearest-neighbor collaborative filtering is used in BPR to learn the anomaly ranking. Unlike item recommendation, in anomaly detection the similarities between positive instances (*i.e.*, anomalies) can be very small, *e.g.*, two anomalies from different anomaly classes, whereas the similarities between negative instances can be rather large, especially in the k -nearest-neighbor region. Thus, BPR is adapted for anomaly detection by enforcing large similarities between negative instances and their nearest neighbors.

4.3 Performance Evaluation Metrics

Each detector yields a ranking of data instances based on the anomaly scores. Two popular and complementary metrics, the Area Under Receiver Operating Characteristic Curve (AUC-ROC) and Area Under Precision-Recall Curve (AUC-PR) (Boyd et al. 2013), are calculated based on the anomaly ranking. AUC-ROC summarizes the ROC curve of true positives against false positives, which often presents an overoptimistic view of the detection performance due to the class-imbalance nature of anomaly detection data; whereas AUC-PR is a summarization of the curve of precision and recall w.r.t. the anomalies, which focuses on the performance on the anomaly class only and is often more practical. A larger AUC-ROC or AUC-PR value reflects better performance. The reported AUC-ROC and AUC-PR are averaged results over 10 independent runs. The paired *Wilcoxon* signed rank (Woolson 2007) using the averaged AUC-ROC (AUC-PR) across multiple datasets (*i.e.*, 12 datasets for known anomalies and 28 datasets for unknown anomalies) is used to examine the statistical significance of the performance of PRO against its competing methods.

4.4 Detection of Known Anomalies

Experiment Settings. We first evaluate the effectiveness of PRO on the 12 real-world datasets with known anomalies. A consistent anomaly contamination rate and the same number of labeled anomalies, is used across all datasets to gain insights into the performance in different real-life applications. Since anomalies are typically rare instances, the anomaly contamination rate is set to 2% by default. The number of labeled anomalies available per data is set to 60, *i.e.*, $|\mathcal{A}| = 60$. We provide the results of PRO on datasets with different amount of labeled data and anomaly contamination rates later in respective Sections 4.6 and 4.7.1.

Table 2 AUC-PR and AUC-ROC Results (mean \pm std). ‘Size’ is the overall data size, D is the dimension. ‘1M’ denotes *news20* has 1,355,191 features. # wins/draws/losses are counted based on whether the mean \pm std performance of PRO outperforms/overlaps/underperforms that of its competing methods.

Data Statistics			AUC-PR Performance						
Data	Size	D	PRO	DevNet	DSVDD	FSNet	cFSNet	BPR	iForest
donors	619,326	10	1.000 \pm 0.000	0.997 \pm 0.005	0.806 \pm 0.110	0.995 \pm 0.004	0.998 \pm 0.001	0.520 \pm 0.030	0.222 \pm 0.035
census	299,285	500	0.356 \pm 0.009	0.345 \pm 0.005	0.330 \pm 0.008	0.197 \pm 0.012	0.197 \pm 0.012	0.173 \pm 0.006	0.078 \pm 0.003
fraud	284,807	29	0.689 \pm 0.004	0.693 \pm 0.004	0.695 \pm 0.004	0.157 \pm 0.024	0.169 \pm 0.040	0.678 \pm 0.003	0.261 \pm 0.035
celeba	202,599	39	0.309 \pm 0.004	0.306 \pm 0.014	0.306 \pm 0.006	0.103 \pm 0.015	0.112 \pm 0.017	0.166 \pm 0.006	0.060 \pm 0.007
dos	109,353	196	0.900 \pm 0.010	0.900 \pm 0.011	0.910 \pm 0.011	0.826 \pm 0.088	0.836 \pm 0.053	0.461 \pm 0.024	0.266 \pm 0.014
rec	106,987	196	0.767 \pm 0.004	0.760 \pm 0.024	0.772 \pm 0.037	0.650 \pm 0.061	0.679 \pm 0.066	0.302 \pm 0.007	0.132 \pm 0.009
fuz	96,000	196	0.170 \pm 0.017	0.136 \pm 0.004	0.133 \pm 0.007	0.146 \pm 0.016	0.146 \pm 0.016	0.075 \pm 0.002	0.039 \pm 0.002
bac	95,329	196	0.890 \pm 0.002	0.863 \pm 0.015	0.862 \pm 0.015	0.618 \pm 0.096	0.618 \pm 0.096	0.117 \pm 0.002	0.050 \pm 0.009
w7a	49,749	300	0.496 \pm 0.008	0.408 \pm 0.029	0.117 \pm 0.024	0.098 \pm 0.005	0.098 \pm 0.005	0.112 \pm 0.013	0.023 \pm 0.001
campaign41,188	62	0.470 \pm 0.008	0.426 \pm 0.008	0.386 \pm 0.014	0.255 \pm 0.017	0.255 \pm 0.017	0.333 \pm 0.010	0.313 \pm 0.022	
news20	10,523	1M	0.652 \pm 0.004	0.632 \pm 0.010	0.329 \pm 0.005	0.105 \pm 0.011	0.116 \pm 0.006	0.222 \pm 0.005	0.035 \pm 0.001
thyroid	7,200	21	0.298 \pm 0.008	0.280 \pm 0.006	0.205 \pm 0.007	0.149 \pm 0.016	0.175 \pm 0.016	0.108 \pm 0.006	0.144 \pm 0.019
Average			0.583	0.562	0.488	0.358	0.367	0.272	0.135
P-value			-	0.005	0.016	0.001	0.001	0.001	0.001
# wins/draws/losses			-	6/6/0	8/4/0	10/2/0	11/1/0	12/0/0	12/0/0

Data Statistics			AUC-PR Performance						
Data	Size	D	PRO	DevNet	DSVDD	FSNet	cFSNet	BPR	iForest
donors	619,326	10	1.000 \pm 0.000	1.000 \pm 0.000	0.993 \pm 0.005	0.999 \pm 0.001	1.000 \pm 0.000	0.976 \pm 0.003	0.875 \pm 0.023
census	299,285	500	0.862 \pm 0.003	0.861 \pm 0.002	0.858 \pm 0.005	0.759 \pm 0.007	0.759 \pm 0.007	0.822 \pm 0.005	0.634 \pm 0.015
fraud	284,807	29	0.980 \pm 0.001	0.981 \pm 0.001	0.980 \pm 0.001	0.776 \pm 0.044	0.762 \pm 0.031	0.974 \pm 0.002	0.946 \pm 0.004
celeba	202,599	39	0.960 \pm 0.001	0.961 \pm 0.002	0.958 \pm 0.001	0.855 \pm 0.014	0.855 \pm 0.030	0.899 \pm 0.003	0.686 \pm 0.021
dos	109,353	196	0.949 \pm 0.007	0.948 \pm 0.007	0.956 \pm 0.005	0.927 \pm 0.019	0.935 \pm 0.013	0.890 \pm 0.006	0.762 \pm 0.018
rec	106,987	196	0.966 \pm 0.001	0.962 \pm 0.004	0.971 \pm 0.005	0.926 \pm 0.009	0.936 \pm 0.012	0.829 \pm 0.011	0.534 \pm 0.022
fuz	96,000	196	0.882 \pm 0.002	0.873 \pm 0.004	0.875 \pm 0.007	0.858 \pm 0.022	0.858 \pm 0.022	0.789 \pm 0.006	0.548 \pm 0.018
bac	95,329	196	0.976 \pm 0.002	0.968 \pm 0.006	0.945 \pm 0.018	0.950 \pm 0.018	0.950 \pm 0.018	0.882 \pm 0.005	0.741 \pm 0.039
w7a	49,749	300	0.883 \pm 0.004	0.882 \pm 0.013	0.802 \pm 0.014	0.767 \pm 0.010	0.767 \pm 0.010	0.733 \pm 0.013	0.413 \pm 0.013
campaign41,188	62	0.880 \pm 0.009	0.858 \pm 0.006	0.803 \pm 0.012	0.684 \pm 0.019	0.684 \pm 0.019	0.740 \pm 0.008	0.723 \pm 0.015	
news20	10,523	1M	0.956 \pm 0.004	0.960 \pm 0.001	0.909 \pm 0.002	0.686 \pm 0.009	0.690 \pm 0.034	0.869 \pm 0.004	0.333 \pm 0.012
thyroid	7,200	21	0.781 \pm 0.001	0.767 \pm 0.002	0.713 \pm 0.007	0.590 \pm 0.014	0.594 \pm 0.010	0.613 \pm 0.003	0.679 \pm 0.014
Average			0.923	0.918	0.897	0.815	0.816	0.835	0.656
P-value			-	0.075	0.025	0.001	0.001	0.001	0.001
# wins/draws/losses			-	3/9/0	5/7/0	9/3/0	9/3/0	12/0/0	12/0/0

Results. The AUC-PR and AUC-ROC results of PRO and its four competing methods on the 12 datasets are shown in Table 2. PRO performs significantly better than, or comparably well to, all competing methods in both metrics across the 12 datasets. In terms of AUC-PR performance, on average, PRO improves all four competing methods by a large margin, *i.e.*, DevNet (3.7%), DSVDD (19.6%), FSNet (54.0%), cFSNet (59.1%), BPR (114.2%) and iForest (331.1%), which are all statistically significant at the 95%/99% confidence level according to the *Wilcoxon* signed rank test results. Particularly, compared to the top two competing methods, PRO significantly outperforms DevNet on six datasets, with improvement ranging from 3%-6% on *census*, *bac*, *news20* and *thyroid* up to 10%-20% on *campaign* and *w7a*, and they perform comparably well on the rest of six datasets; PRO performs significantly

better than DSVDD on eight datasets, achieving 20%-320% improvement on six datasets, including *donors*, *fuz*, *w7a*, *campaign*, *news20* and *thyroid*, and they perform comparably well on the rest of four datasets. PRO performs significantly better than FSNetm cFSNet, BPR and iForest on 10-12 datasets. In terms of AUC-ROC, PRO performs marginally better than DSVDD (2.9%), FSNet (11.7%), cFSNet (13.1%), BPR (10.6%) and iForest (40.7%) at the 95%/99% confidence level.

The superiority of PRO here is mainly due to that, as discussed in Section 3.1, the pairing data augmentation substantially extends the supervision information of known anomalies through pairwise interaction. As a result, PRO can gain substantial improvement over its contenders when the interaction between $C_{\{a,a\}}/C_{\{a,u\}}/C_{\{u,u\}}$ instance pairs contributes supervision information that cannot be learned using the individual labeled anomaly data. Additionally, the end-to-end anomaly score learning also enables PRO (as well as DevNet) to make more effective use of the labeled data than the two-step method DSVDD that first feature representations and then calculate anomaly scores based on the new representations. The few-shot binary classifier FSNet and its cost-sensitive variant cFSNet attempt to learn expressive prototypical representations of both normal and abnormal classes, but the limited amount of labeled anomaly data prevents them from learning generalized representations, especially for the anomaly class. FSNet and cFSNet can work well on datasets where normal and anomaly classes are well separable and the intra-class variation in both classes are small, such as *donors*, *dos*, *rec* and *bac* on which most detectors achieve very good AUC-ROC and AUC-PR performance. However, they become ineffective in other challenging datasets where anomalies may arbitrarily distribute and are difficult to be distinguished from normal data instances. BPR is designed to optimize AUC-ROC performance and it performs fairly well in AUC-ROC but ineffectively in AUC-PR. The labeled data here is significantly less than that as in collaborative filtering for which BPR is originally proposed. This may substantially limit the performance of BPR.

Note that the performance difference in AUC-PR is far more substantial than that in AUC-ROC in Table 2. This demonstrates the fact that AUC-ROC ignores the detection recall rate of the anomaly class and is considerably less sensitive to the performance of detecting anomalies than AUC-PR, so it shows overoptimistic performance in terms of successfully detecting all anomalies. On the other hand, due to the rareness of anomalies, it is typically very challenging to obtain good AUC-PR performance, *e.g.*, having an AUC-PR performance of greater than 0.7. This explains the large gaps between the average AUC-PR and AUC-ROC results, and also indicates the significance for PRO to achieve more substantially improved AUC-PR performance than AUC-ROC performance.

4.5 Detection of Unknown Anomalies

Experiment Settings. This section evaluates the generalizability of PRO in detecting unknown anomalies on the other 28 datasets. Similar to the settings in Section 4.4, the anomaly contamination rate of 2% and $|\mathcal{A}| = 60$ are also used here. The competing method iForest also performs poorly here and is left out for brevity.

Results. The AUC-PR and AUC-ROC performance of PRO and the five top competing methods on the 28 datasets are presented in Table 3. The results show that PRO outperforms the five competing methods all by substantial margins in detecting unknown anomalies on the 28 datasets. On average, very impressively, PRO improves DevNet by more than 11%, DSVDD by 17%, FSNet by 30%, cFSNet by 20% and BPR by 27% in AUC-PR. It is very

encouraging that, compared to the best competing method DevNet, PRO achieves 20%-130% AUC-PR improvement on eight datasets, including 20%-40% improvement on ' $rec \rightarrow bac$ ', ' $rec, fuz \rightarrow dos$ ', ' $rec, bac, fuz \rightarrow dos$ ', ' $bac, fuz \rightarrow dos$ ', ' $fuz \rightarrow dos$ ', ' $rec, bac, dos \rightarrow fuz$ ', and over 100% improvement on ' $rec, fuz \rightarrow bac$ ' and ' $fuz \rightarrow bac$ '. The improvement of PRO over the other four competing methods is much more substantial than that of PRO over DevNet, *e.g.*, PRO gains 21 wins and 6 draws against DSVDD, 25 wins and 3 draws against FSNet, 24 wins and 3 draws against cFSNet, and 21 wins and 2 draws against BPR. The p-values from the paired *Wilcoxon* signed rank test show that PRO significantly outperforms all three competing methods at the 99% confidence level. Due to the same reason as in the results of detecting known anomalies in Table 2, the AUC-ROC improvement of PRO over the competing methods is less than that in the improvement of AUC-PR, but it is also statistically significant at the 99% confidence level, averagely outperforming DevNet by 2.5%, DSVDD by 11%, FSNet by 8%, cFSNet by 5%, and BPR by 7.5%.

These large evaluation results justify the superior improvement of PRO in generalizing from a few labeled anomalies to detect unknown anomalies. The competing methods may have overfitting of the small labeled anomaly set \mathcal{A} , whereas the substantially augmented data well generalizes PRO, enabling PRO to effectively avoid/reduce the potential overfitting. Also, the ternary representations of normality and abnormality in PRO are more expressive than DevNet, DSVDD, FSNet, cFSNet, and BPR that are built upon single normality, or binary normality and abnormality representations. These unique characteristics make PRO stand out particularly in complex datasets such as ' $rec \rightarrow bac$ ', ' $rec, fuz \rightarrow bac$ ', ' $rec, fuz \rightarrow dos$ ' and ' $rec, bac, fuz \rightarrow dos$ ', on which PRO achieves good/excellent AUC-PR performance against pair/poor AUC-PR performance of all three competing methods. Additionally, due to these characteristics PRO generally performs more stably than its competing methods, as illustrated by its smaller standard deviation of AUC-PR/AUC-ROC results.

DSVDD substantially outperforms PRO on one dataset, ' $bac \rightarrow dos$ ', on which all detectors obtain excellent AUC-PR performance with DSVDD achieving a nearly perfect AUC-PR result, *i.e.*, an AUC-PR of 0.961. This indicates this dataset is very simple. The availability of a few known bac attacks is sufficient to learn an excellent one-class hyperplane detect almost all of the unknown dos attacks. In such simple cases simpler models like DSVDD and DevNet may be better choices. PRO also has one lose to DevNet on the dataset ' $rec, dos \rightarrow fuz$ '. This may be because the Gaussian prior DevNet makes on the anomaly scores fits this dataset very well, enabling it to learn better anomaly scores than PRO. BPR obtains five wins over PRO on the five most challenging datasets, *i.e.*, ' $fuz \rightarrow dos$ ', ' $dos \rightarrow fuz$ ', ' $dos, bac \rightarrow fuz$ ', ' $rec, bac, dos \rightarrow fuz$ ' and ' $rec, dos \rightarrow fuz$ ', where PRO and the other four competing methods cannot achieve similarly good performance as on the other datasets. We conjecture that this is due to that the pairwise AUC optimization in BPR helps learn representations with larger margins between normal and abnormal data.

4.6 Availability of Known Anomalies

Experiment Settings. This section examines how effective PRO can leverage the limited amount of labeled anomaly data by inspecting its performance w.r.t. different number of labeled anomalies, ranging from 15 to 120, with the contamination rate fixed to 2%. The experiments are performed on datasets containing known and unknown anomalies. Since there are too many unknown anomaly datasets to well present all the results, only the results on half of unknown anomaly datasets are reported here. DevNet, DSVDD, FSNet, cFSNet

Table 3 AUC-PR and AUC-ROC Results (mean \pm std) on Detecting Unknown Anomalies. The models are trained with the labeled data from known anomaly classes to detect unknown anomalies. # wins/draws/losses are counted based on whether the mean \pm std performance of PRO outperforms/overlaps/underperforms that of its competing methods.

Anomaly Class		AUC-PR					
Known	Unknown	PRO	DevNet	DSVDD	FSNet	cFSNet	BPR
dos	bac	0.908 \pm 0.005	0.908 \pm 0.005	0.890 \pm 0.008	0.772 \pm 0.129	0.841 \pm 0.053	0.590 \pm 0.025
dos, fuz	bac	0.889 \pm 0.003	0.886 \pm 0.002	0.879 \pm 0.009	0.555 \pm 0.099	0.679 \pm 0.035	0.438 \pm 0.009
fuz	bac	0.503 \pm 0.042	0.219 \pm 0.015	0.266 \pm 0.075	0.366 \pm 0.153	0.524 \pm 0.086	0.500 \pm 0.003
rec	bac	0.752 \pm 0.006	0.541 \pm 0.062	0.583 \pm 0.032	0.55 \pm 0.158	0.637 \pm 0.042	0.474 \pm 0.011
rec, dos	bac	0.834 \pm 0.006	0.845 \pm 0.013	0.833 \pm 0.006	0.480 \pm 0.118	0.537 \pm 0.047	0.548 \pm 0.043
rec, dos, fuz	bac	0.706 \pm 0.016	0.631 \pm 0.033	0.623 \pm 0.034	0.368 \pm 0.166	0.368 \pm 0.166	0.500 \pm 0.011
rec, fuz	bac	0.711 \pm 0.014	0.342 \pm 0.065	0.317 \pm 0.102	0.312 \pm 0.088	0.387 \pm 0.072	0.436 \pm 0.010
bac	dos	0.938 \pm 0.012	0.943 \pm 0.011	0.961 \pm 0.008	0.930 \pm 0.013	0.944 \pm 0.007	0.769 \pm 0.006
bac, fuz	dos	0.932 \pm 0.001	0.761 \pm 0.031	0.772 \pm 0.028	0.714 \pm 0.092	0.803 \pm 0.040	0.801 \pm 0.009
fuz	dos	0.811 \pm 0.007	0.644 \pm 0.040	0.680 \pm 0.074	0.774 \pm 0.055	0.803 \pm 0.069	0.846 \pm 0.003
rec	dos	0.928 \pm 0.002	0.846 \pm 0.012	0.855 \pm 0.010	0.798 \pm 0.062	0.831 \pm 0.030	0.771 \pm 0.005
rec, bac	dos	0.891 \pm 0.008	0.870 \pm 0.016	0.871 \pm 0.013	0.686 \pm 0.067	0.762 \pm 0.075	0.742 \pm 0.014
rec, bac, fuz	dos	0.835 \pm 0.007	0.610 \pm 0.036	0.699 \pm 0.053	0.572 \pm 0.066	0.627 \pm 0.087	0.641 \pm 0.002
rec, fuz	dos	0.883 \pm 0.004	0.718 \pm 0.030	0.673 \pm 0.039	0.670 \pm 0.096	0.764 \pm 0.042	0.749 \pm 0.004
bac	fuz	0.418 \pm 0.008	0.420 \pm 0.017	0.250 \pm 0.011	0.374 \pm 0.030	0.383 \pm 0.025	0.251 \pm 0.003
dos	fuz	0.418 \pm 0.014	0.427 \pm 0.026	0.325 \pm 0.020	0.288 \pm 0.037	0.324 \pm 0.038	0.476 \pm 0.015
dos, bac	fuz	0.375 \pm 0.007	0.371 \pm 0.008	0.322 \pm 0.016	0.273 \pm 0.021	0.301 \pm 0.015	0.463 \pm 0.012
rec	fuz	0.462 \pm 0.003	0.418 \pm 0.014	0.419 \pm 0.008	0.410 \pm 0.032	0.427 \pm 0.022	0.408 \pm 0.007
rec, bac	fuz	0.315 \pm 0.005	0.311 \pm 0.013	0.314 \pm 0.009	0.260 \pm 0.025	0.255 \pm 0.020	0.319 \pm 0.018
rec, bac, dos	fuz	0.294 \pm 0.006	0.246 \pm 0.004	0.249 \pm 0.001	0.206 \pm 0.024	0.189 \pm 0.017	0.349 \pm 0.013
rec, dos	fuz	0.349 \pm 0.012	0.375 \pm 0.007	0.366 \pm 0.014	0.276 \pm 0.030	0.306 \pm 0.018	0.434 \pm 0.003
bac	rec	0.892 \pm 0.012	0.890 \pm 0.016	0.576 \pm 0.069	0.689 \pm 0.049	0.718 \pm 0.058	0.592 \pm 0.008
bac, fuz	rec	0.876 \pm 0.004	0.804 \pm 0.042	0.831 \pm 0.031	0.672 \pm 0.065	0.692 \pm 0.042	0.554 \pm 0.015
dos	rec	0.849 \pm 0.012	0.846 \pm 0.016	0.739 \pm 0.017	0.615 \pm 0.048	0.718 \pm 0.074	0.686 \pm 0.006
dos, bac	rec	0.768 \pm 0.010	0.732 \pm 0.011	0.670 \pm 0.023	0.618 \pm 0.056	0.644 \pm 0.031	0.597 \pm 0.013
dos, bac, fuz	rec	0.719 \pm 0.022	0.716 \pm 0.022	0.629 \pm 0.020	0.540 \pm 0.035	0.586 \pm 0.025	0.447 \pm 0.016
dos, fuz	rec	0.788 \pm 0.010	0.772 \pm 0.010	0.615 \pm 0.018	0.631 \pm 0.035	0.644 \pm 0.017	0.542 \pm 0.007
fuz	rec	0.797 \pm 0.022	0.718 \pm 0.042	0.727 \pm 0.060	0.760 \pm 0.045	0.785 \pm 0.013	0.672 \pm 0.003
Average		0.709	0.636	0.605	0.542	0.589	0.557
P-value		-	0.001	0.000	0.000	0.000	0.000
# wins/draws/losses		-	14/13/1	21/6/1	25/3/0	24/4/0	21/2/5

Anomaly Class		AUC-ROC					
Known	Unknown	PRO	DevNet	DSVDD	FSNet	cFSNet	BPR
dos	bac	0.958 \pm 0.002	0.956 \pm 0.006	0.924 \pm 0.010	0.932 \pm 0.021	0.943 \pm 0.012	0.889 \pm 0.005
dos, fuz	bac	0.969 \pm 0.003	0.967 \pm 0.004	0.918 \pm 0.011	0.921 \pm 0.016	0.941 \pm 0.011	0.886 \pm 0.003
fuz	bac	0.869 \pm 0.004	0.794 \pm 0.009	0.812 \pm 0.029	0.872 \pm 0.050	0.896 \pm 0.031	0.899 \pm 0.001
rec	bac	0.965 \pm 0.000	0.900 \pm 0.012	0.902 \pm 0.013	0.885 \pm 0.063	0.921 \pm 0.014	0.846 \pm 0.014
rec, dos	bac	0.977 \pm 0.002	0.980 \pm 0.002	0.978 \pm 0.001	0.924 \pm 0.016	0.942 \pm 0.005	0.882 \pm 0.011
rec, dos, fuz	bac	0.971 \pm 0.002	0.953 \pm 0.008	0.952 \pm 0.017	0.916 \pm 0.030	0.916 \pm 0.030	0.886 \pm 0.007
rec, fuz	bac	0.969 \pm 0.001	0.891 \pm 0.010	0.890 \pm 0.021	0.865 \pm 0.024	0.902 \pm 0.014	0.874 \pm 0.000
bac	dos	0.906 \pm 0.024	0.915 \pm 0.021	0.945 \pm 0.011	0.926 \pm 0.013	0.933 \pm 0.010	0.881 \pm 0.010
bac, fuz	dos	0.958 \pm 0.000	0.889 \pm 0.013	0.887 \pm 0.014	0.872 \pm 0.033	0.911 \pm 0.013	0.924 \pm 0.002
fuz	dos	0.855 \pm 0.002	0.792 \pm 0.018	0.805 \pm 0.028	0.826 \pm 0.037	0.846 \pm 0.042	0.921 \pm 0.002
rec	dos	0.938 \pm 0.002	0.883 \pm 0.008	0.887 \pm 0.006	0.825 \pm 0.037	0.846 \pm 0.032	0.875 \pm 0.007
rec, bac	dos	0.944 \pm 0.003	0.932 \pm 0.006	0.931 \pm 0.005	0.872 \pm 0.029	0.887 \pm 0.033	0.904 \pm 0.006
rec, bac, fuz	dos	0.940 \pm 0.002	0.861 \pm 0.008	0.886 \pm 0.023	0.821 \pm 0.021	0.858 \pm 0.023	0.890 \pm 0.005
rec, fuz	dos	0.939 \pm 0.001	0.874 \pm 0.011	0.868 \pm 0.010	0.834 \pm 0.043	0.880 \pm 0.018	0.903 \pm 0.003
bac	fuz	0.752 \pm 0.014	0.743 \pm 0.030	0.364 \pm 0.059	0.697 \pm 0.072	0.734 \pm 0.054	0.695 \pm 0.010
dos	fuz	0.708 \pm 0.030	0.737 \pm 0.049	0.508 \pm 0.045	0.606 \pm 0.094	0.708 \pm 0.058	0.783 \pm 0.019
dos, bac	fuz	0.842 \pm 0.012	0.833 \pm 0.010	0.646 \pm 0.065	0.837 \pm 0.029	0.860 \pm 0.009	0.828 \pm 0.006
rec	fuz	0.878 \pm 0.005	0.872 \pm 0.001	0.872 \pm 0.002	0.843 \pm 0.023	0.838 \pm 0.028	0.777 \pm 0.010
rec, bac	fuz	0.879 \pm 0.006	0.879 \pm 0.001	0.880 \pm 0.002	0.838 \pm 0.034	0.824 \pm 0.015	0.797 \pm 0.012
rec, bac, dos	fuz	0.885 \pm 0.002	0.878 \pm 0.001	0.878 \pm 0.001	0.846 \pm 0.018	0.853 \pm 0.013	0.832 \pm 0.013
rec, dos	fuz	0.850 \pm 0.014	0.889 \pm 0.005	0.871 \pm 0.028	0.822 \pm 0.021	0.837 \pm 0.023	0.800 \pm 0.010
bac	rec	0.928 \pm 0.007	0.926 \pm 0.014	0.489 \pm 0.099	0.693 \pm 0.096	0.713 \pm 0.110	0.741 \pm 0.012
bac, fuz	rec	0.958 \pm 0.002	0.943 \pm 0.011	0.947 \pm 0.009	0.879 \pm 0.017	0.897 \pm 0.011	0.822 \pm 0.008
dos	rec	0.867 \pm 0.018	0.865 \pm 0.025	0.677 \pm 0.030	0.636 \pm 0.083	0.727 \pm 0.086	0.778 \pm 0.008
dos, bac	rec	0.908 \pm 0.008	0.891 \pm 0.005	0.724 \pm 0.037	0.859 \pm 0.035	0.868 \pm 0.015	0.805 \pm 0.012
dos, bac, fuz	rec	0.907 \pm 0.005	0.907 \pm 0.007	0.820 \pm 0.039	0.871 \pm 0.014	0.892 \pm 0.015	0.783 \pm 0.014
dos, fuz	rec	0.899 \pm 0.013	0.885 \pm 0.011	0.663 \pm 0.026	0.842 \pm 0.037	0.863 \pm 0.005	0.800 \pm 0.011
fuz	rec	0.890 \pm 0.008	0.855 \pm 0.021	0.863 \pm 0.023	0.871 \pm 0.031	0.885 \pm 0.008	0.812 \pm 0.003
Average		0.904	0.882	0.814	0.837	0.861	0.840
P-value		-	0.001	0.000	0.000	0.000	0.000
# wins/draws/losses		-	14/13/1	20/7/1	18/10/0	18/10/0	24/1/3

and BPR are used as competing methods. The unsupervised method iForest is insensitive to the labeled data and used as the baseline.

Note that since AUC-PR results are much more indicative than AUC-ROC results, we focus on the AUC-PR performance hereafter.

Results. The AUC-PR results on the 12 known anomaly datasets are shown in Fig. 2. The performance of all deep methods generally increases with increasing labeled data. However, The increased anomalies do not always help due to the heterogeneous anomalous behaviors taken by different anomalies. PRO is more stable in the increasing trend. Consistent to that the results in Table 2, PRO still significantly outperforms its state-of-the-art competing methods when the availability of known anomalies changes. Note that compared to FSNet, cFSNet and BPR, the other three methods - PRO, DevNet and DSVDD - can leverage the increased labeled anomaly data much better. This may due to that the objective function of PRO, DevNet and DSVDD are more customized to the studied setting than FSNet, cFSNet and BPR that are adapted from other learning tasks rather than anomaly detection.

Particularly, PRO demonstrates the most data-efficient learning capability. Impressively, PRO can be trained with 50%-75% less labeled anomalies but achieves much better, or comparably good, AUC-PR than the best contender DevNet on multiple datasets like *dos*, *fuz*, *w7a* and *campaign*; and it is trained with 87.5% less labeled data while obtains substantially better performance than the second best contender DSVDD on *donors*, *w7a*, *campaign*, *news20* and *thyroid*. The same observation applies to FSNet, cFSNet and BPR on most of the 12 datasets. We believe the pairing data augmentation is the main driving force for the substantially improved data efficiency of PRO.

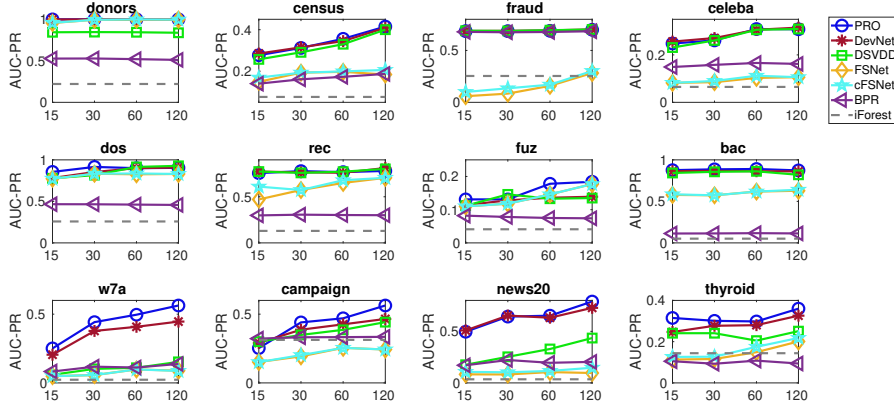


Fig. 2 AUC-PR Performance w.r.t. the Number of Labeled Anomalies

Fig. 3 presents the AUC-PR results on the 14 unknown anomaly datasets. The performance of PRO here is consistent to that in Table 2. PRO remains to be the most data-efficient learning method, and can perform substantially better than the best competing methods even when the PRO model is trained with 50%-87.5% less labeled data.

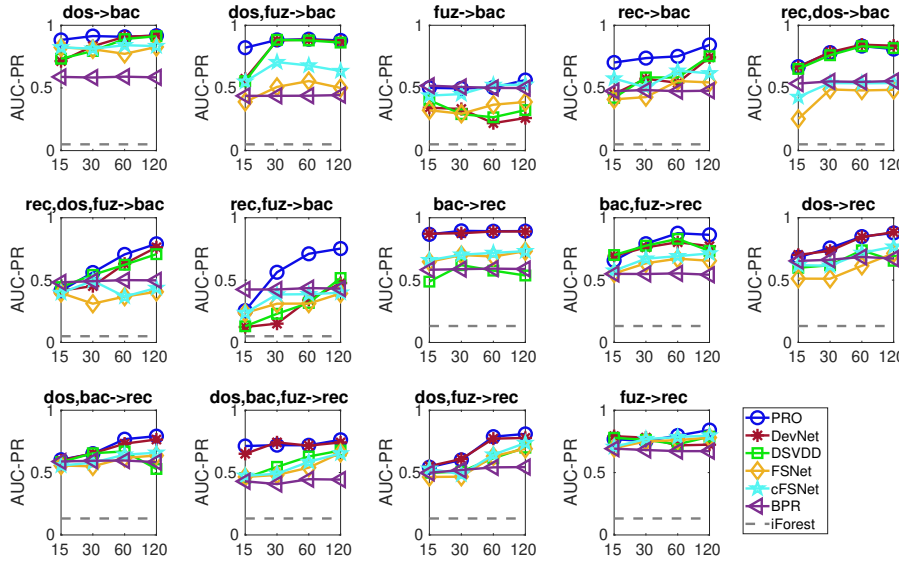


Fig. 3 AUC-PR Performance of Detecting Unknown Anomalies Using Different Number of Labeled Anomalies. ‘A -> B’ means that the models are trained with labeled attacks ‘A’ to detect unknown attacks ‘B’.

4.7 Further Analysis of PRO

This section inspects some intrinsic behaviors of PRO. Since the findings on the known and unknown anomaly datasets are similar, here we focus on the 12 known anomaly datasets.

4.7.1 Tolerance to Anomaly Contamination in Unlabeled Data

Experiment Settings. We examine the robustness w.r.t. different anomaly contamination rates, $\{0\%, 2\%, 5\%, 10\%\}$, with the number of labeled anomalies fixed to 60. The case with 0% contamination rate is used as the baseline.

Results. The AUC-PR results of PRO w.r.t. different contamination rates are presented in Fig. 5. As expected in our theoretical analysis in Section 3.2, PRO performs very well and stably on all datasets when the contamination rate is reasonably small, *e.g.*, 2%-5%. It is very impressive that this trend remains on nearly all datasets except *census*, *w7a* and *news20*, even when the rate increases to 10%. This robustness is due to two main reasons: (i) the regression modeling itself is tolerant to a certain proportion of outliers, and (ii) our theoretical analysis suggests that in PRO true anomalies are expected to be assigned with larger anomaly scores than normal instances for small anomaly contamination.

4.7.2 Ablation Study

Experiment Settings. PRO is compared with the following four ablated variants to examine the importance of its key individual components:

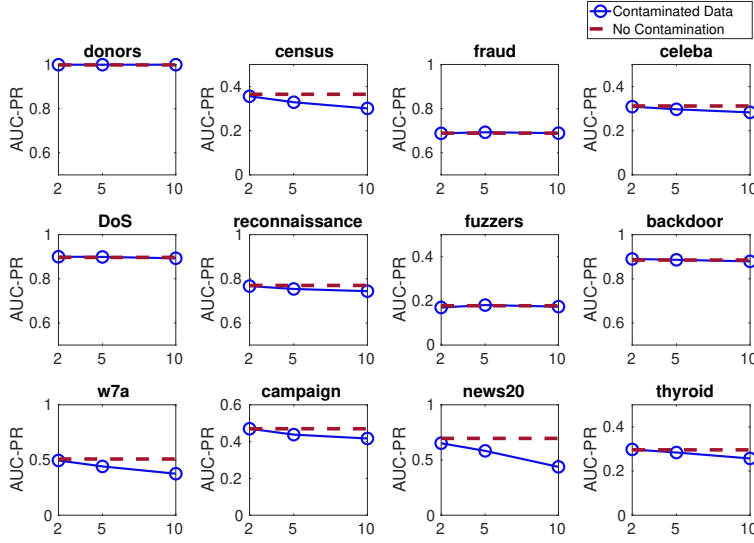


Fig. 4 AUC-PR Performance of PRO on Data of Different Contamination Rates (%). The PRO’s performance on data with no anomaly contamination is used as the baseline.

- **BOR.** BOR reduces PRO from ternary ordinal regression to Binary Ordinal Regression (BOR) by merging the two anomaly-related synthetic class labels $y_{\{a,a\}} = 8$ and $y_{\{a,u\}} = 4$ into one label $y_{\{a,a\}|\{a,u\}} = 4$, with the class $y_{\{u,u\}} = 0$ unchanged.
- **OSNet.** OSNet is a simplified PRO that is reduced from a two-stream neural network to a One-Stream neural Network (OSNet), which means OSNet takes single data points as inputs rather than pairs of data points in PRO. In other words, OSNet discards the pairing-based data augmentation in PRO. Also, for single data points, we can only have two possible synthetic class labels y_a and y_u . Therefore, OSNet trains a binary ordinal regression model with $y_a = 4$ and $y_u = 0$.
- **LDM.** LDM removes the hidden layers of PRO and learns a Linear Direct Mapping (LDM) from the original data space to anomaly scores.
- **A2H.** A2H is a variant having more complex network architecture than PRO, which deepens PRO with additional two hidden (A2H) layers. ℓ_2 -norm regularizer is also added to these hidden layers to avoid overfitting.

Results. The ablation study results are shown in Table 4. The results show that PRO performs substantially better than its four variants by large improvement margins, *i.e.*, BOR (5.6%), OSNet (3.7%), LDM (11.0%) and A2H (3.3%). The improvement over BOR and OSNet are statistically significant at the 99% confidence level. This justifies that both of the pairing data augmentation and ternary ordinal regression makes significant contribution to the performance of PRO. On the other hand, it is impressive that even BOR and OSNet are the simplified variants of PRO, they perform comparably well to the best state-of-the-art competing method DevNet in Table 2. Eliminating the feature representation layer, *i.e.*, the ψ function, from PRO results in LDM, which also performs significantly worse than PRO, with over 10% loss in the average AUC-PR performance, indicating the critical role of the intermediate representation learning in PRO. Compared to the variant with a deeper architecture, A2H, although PRO achieves large average improvement, the improvement is not statistically significant across the datasets. This is because the deeper architecture can help

achieve significant AUC-PR gains on some datasets like *rec* and *thyroid*, but significantly deteriorates on most of the other datasets. Thus, the default network architecture used in PRO is generally recommended.

Table 4 AUC-PR Performance of PRO and Its Four Ablated Variants.

Data	PRO	BOR	OSNet	LDM	A2H
donors	1.000 \pm 0.000	0.995 \pm 0.011	0.999 \pm 0.002	0.974 \pm 0.023	1.000 \pm 0.000
census	0.356 \pm 0.009	0.324 \pm 0.010	0.325 \pm 0.011	0.355 \pm 0.001	0.283 \pm 0.035
fraud	0.689 \pm 0.004	0.692 \pm 0.008	0.701 \pm 0.008	0.662 \pm 0.004	0.708 \pm 0.004
celeba	0.309 \pm 0.004	0.308 \pm 0.007	0.299 \pm 0.016	0.294 \pm 0.005	0.299 \pm 0.007
dos	0.900 \pm 0.010	0.887 \pm 0.003	0.887 \pm 0.005	0.839 \pm 0.003	0.877 \pm 0.015
rec	0.767 \pm 0.004	0.751 \pm 0.016	0.750 \pm 0.015	0.647 \pm 0.005	0.877 \pm 0.005
fuz	0.170 \pm 0.017	0.147 \pm 0.009	0.151 \pm 0.008	0.163 \pm 0.004	0.178 \pm 0.015
bac	0.890 \pm 0.002	0.879 \pm 0.006	0.879 \pm 0.007	0.805 \pm 0.012	0.863 \pm 0.008
w7a	0.496 \pm 0.008	0.467 \pm 0.015	0.482 \pm 0.011	0.406 \pm 0.002	0.415 \pm 0.016
campaign	0.470 \pm 0.008	0.423 \pm 0.010	0.402 \pm 0.010	0.406 \pm 0.003	0.246 \pm 0.042
news20	0.652 \pm 0.004	0.481 \pm 0.004	0.625 \pm 0.004	0.552 \pm 0.001	0.618 \pm 0.023
thyroid	0.298 \pm 0.008	0.269 \pm 0.013	0.248 \pm 0.011	0.201 \pm 0.015	0.411 \pm 0.015
Average	0.583	0.552	0.562	0.525	0.565
P-value	-	0.002	0.003	0.001	0.413

4.7.3 Sensitivity w.r.t. Ordinal Class Labels

Experiment Settings. This section examines the sensitivity of PRO w.r.t. the pre-defined synthetic ordinal class labels. We fix the ordinal label for $C_{\{u,u\}}$ to be zero, *i.e.*, $c_3 = 0$, and the same margin is set between $C_{\{u,u\}} - C_{\{a,u\}}$ pairs and between $C_{\{a,u\}} - C_{\{a,a\}}$ pairs, *i.e.*, $(c_2 - c_3) = (c_1 - c_2) = m$. We test the sensitivity w.r.t. different values of the margin m .

Results. The AUC-PR results are shown in Figure 5. It is clear that PRO is generally robust to different margin values. PRO performs well even when setting a rather small margin, *e.g.*, $m = 0.25$. This may imply that the ordinal regression in PRO can be optimized to well discriminate the random pairs of samples. Large margins are desired in some challenging datasets such as *thyroid* and *dos*. However, PRO may overfit the data when a large margin is used, *e.g.*, $m = 8$, leading to some decline in the performance on a few datasets such as *donors*, *campaign* and *news20*. Thus, a medium margin $m = 4$ is generally recommended.

4.7.4 Sensitivity w.r.t. Ensemble Size E

Experiment Settings. This section investigates the sensitivity of PRO w.r.t. the ensemble size E in Eqn. (6). A wide range of ensemble sizes $E = \{1, 10, 20, 30, 40, 50\}$ is evaluated.

Results. The AUC-PR results using different ensemble sizes are shown in Figure 5. PRO performs very stably across all the 12 datasets. PRO using $E = 1$ performs similarly well as that using a larger E . This indicates that PRO can pair test instances with single randomly selected training instances to well distinguish three categories of random pairs. Increasing E may offer better detection accuracy on some datasets such as *fuz* and *thyroid*, but the improvement is often marginal.

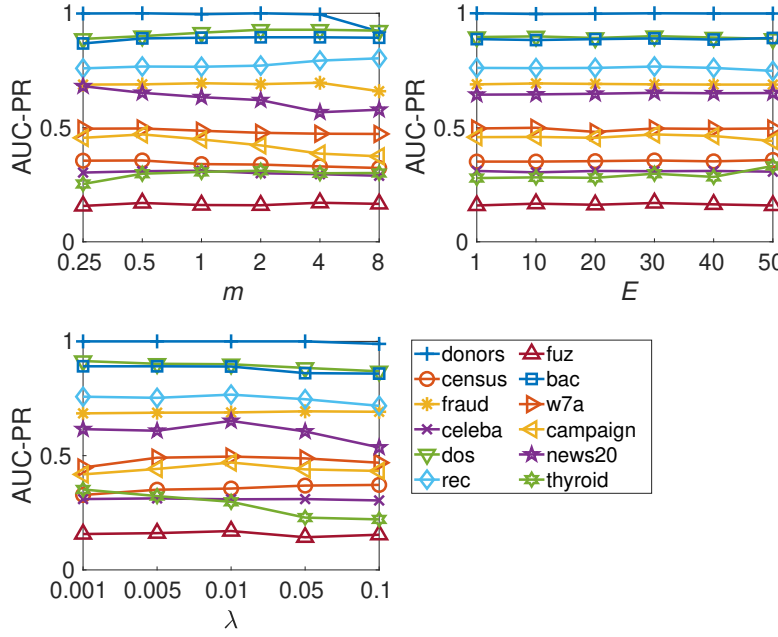


Fig. 5 AUC-PR Performance of PRO w.r.t. Different m , E and λ . m is the margin between synthetic ordinal labels, E is the number of random pairs used in the inference, and λ is the regularization parameter.

4.7.5 Sensitivity w.r.t. Regularization Parameter λ

Experiment Settings. This section investigates the sensitivity of PRO w.r.t. the regularization parameter λ as in Eqn. (5). A wide range of settings $\lambda = \{0.001, 0.005, 0.01, 0.05, 0.1\}$ is evaluated.

Results. The AUC-PR results using different λ settings are shown in Figure 5. The performance of PRO is generally robust w.r.t. different λ values on all the 12 datasets, especially when λ is chosen in the range $[0.001, 0.01]$. When increasing λ to larger values such as 0.05 or 0.1, the AUC-PR of PRO decreases on a few datasets, *e.g.*, *rec*, *bac*, *news20* and *thyroid*. This may due to that given the limited number of labeled anomaly data, enforcing strong model regularization in PRO can lead to underfitting on those datasets. Therefore, a small λ , *e.g.*, $\lambda = 0.01$, is generally recommended in our weakly-supervised setting.

5 Related Work

5.1 Deep Anomaly Detection

Traditional anomaly detection approaches are often ineffective in high-dimensional or non-linear separable data due to the curse of dimensionality and the deficiency in capturing the non-linear relations (Aggarwal 2017). Deep anomaly detection has shown promising results in handle those complex data (Pang et al. 2020), of which most methods are based on autoencoders (Hawkins et al. 2002; Chen et al. 2017) or generative adversarial networks (Schlegl et al. 2017; Zenati et al. 2018). These methods generally follow a two-step ap-

proach. They often first learn new representations of the data and use the reconstruction loss from the new representation space as anomaly score. One issue with these methods is that the learned representations are primarily optimized to represent the whole data rather than to detect anomalies. Some very recent methods (Zong et al. 2018; Pang et al. 2018; Ruff et al. 2018; Zheng et al. 2019) address this issue by learning representations tailored for specific anomaly measures, *e.g.* cluster membership-based measure in (Zong et al. 2018), distance-based measure in (Pang et al. 2018) and one-class classification-based measure in (Ruff et al. 2018; Chalapathy et al. 2018; Zheng et al. 2019; Ruff et al. 2019). However, they still focus on optimizing the feature representations. By contrast, PRO unifies representation learning and anomaly scoring into one pipeline to directly optimize anomaly scores, yielding more optimized anomaly scores. A number of other deep anomaly detection approaches can be found in the recent survey paper (Pang et al. 2020).

5.2 Weakly- and Semi-supervised Anomaly Detection

Many studies have been introduced to leverage labeled normal instances to learn patterns of the normal class, which are commonly referred to as semi-supervised anomaly detection methods (Noto et al. 2012; Görmitz et al. 2013; Ienco et al. 2017). The semi-supervised setting is relevant to our problem because of the availability of both labeled and unlabeled data, but they are two different tasks due to the difference in training data and the problem nature. Specifically, we have only a few labeled anomaly data rather than large-scale labeled normal data; and the anomalies are often from different distributions or manifolds, so having only limited labeled anomaly data hardly cover all types of anomalies. Therefore, instead of modeling the labeled normal data, our problem requires to learn patterns of labeled anomalies that also generalize well to unseen anomalies. A few studies (McGlohon et al. 2009; Tamersoy et al. 2014; Zhang et al. 2018; Pang et al. 2018) show that these limited labeled anomalies can be leveraged to substantially improve the detection accuracy. However, these studies exploit the labeled anomalies to enhance anomaly scoring via label propagation (McGlohon et al. 2009; Tamersoy et al. 2014; Vercruyssen et al. 2018), representation learning (Pang et al. 2018) or classification models (Zhang et al. 2018), failing to sufficiently utilize the labeled data and/or detect unseen anomalies. Ruff et al. (2019) studies a partly similar problem to ours. One key difference is that a small set of both labeled anomalies and normal instances are assumed to be available in (Ruff et al. 2019), while we only assume the availability of a few labeled anomalies. They address the problem by extending DSVDD with an additional term into the SVDD objective function to guarantee the large (small) margin between the one-class center and labeled anomalies (normal instances). The adaptive DSVDD used in our comparison shares a similar spirit to this extended DSVDD. Our previous work DevNet (Pang et al. 2019) addresses the same problem as this work, but DevNet and PRO represents two completely different approaches. PRO is based on a pairwise relation learning task and learns anomaly scores using deep ternary ordinal regression with no distribution assumption on anomaly scores, whereas DevNet is a Gaussian prior-driven score learning approach that optimizes the anomaly scores by fitting to a Z-Score-based distribution.

This research line is also relevant to few-shot classification (Fei-Fei et al. 2006; Vinyals et al. 2016; Snell et al. 2017) and positive and unlabeled data (PU) learning (Li and Liu 2003; Elkan and Noto 2008; Sansone et al. 2018) because of the availability of the limited labeled positive instances (anomalies), but they are very different in that these two areas implicitly assume that the few labeled instances share the same intrinsic class structure as the other instances within the same class (*e.g.*, the anomaly class), whereas the few labeled anomalies

and the unknown anomalies may have diverse class structures. This presents significant challenges to the techniques of both areas.

5.3 AUC Optimization

Area under the ROC curve (AUC-ROC) optimization, which aims at maximizing the AUC-ROC value of a ranking of data instances, is another related research line. Our method aims to learn larger anomaly scores to anomalies than normal instances such that anomalies are top-ranked in the returned anomaly ranking list. This has a similar motivation to the AUC-ROC optimization problem that optimizes an instance ranking such that a given positive instance is ranked higher than any negative instances. Several other semi-supervised anomaly detectors, such as semi-supervised DSVDD (Ruff et al. 2019) and DevNet (Pang et al. 2019), also share this general objective. One key difference is that these anomaly detection studies focus on point-wise anomaly score learning, and they do not explicitly enforce an overall high true positive rate as in related AUC optimization studies (Cortes and Mohri 2004; Calders and Jaroszewicz 2007; Gao and Zhou 2015; Grabocka et al. 2019) (or area under the precision-recall curve (AUC-PR) optimization (Eban et al. 2017; Mohapatra et al. 2014)). Different from ranking problems in information retrieval, there are two unique challenges in anomaly detection: (i) unseen positive instances can be completely different from the given positive instances, such as unknown anomalies, resulting in significantly high and irregular class variation; and (ii) there is often only very limited amount of labeled anomaly data. This renders direct AUC-ROC or AUC-PR optimization approaches less effective in anomaly detection.

6 Conclusions and Discussions

This paper introduces a novel formulation and its instantiation to devise two-stream ordinal regression neural networks for deep weakly-supervised anomaly detection. Our approach achieves significant improvement over six state-of-the-art competing methods in detecting both known and unknown anomalies and data efficiency. This well justifies our approach’s capability in generalizing from a few labeled anomalies and its tolerance to anomaly contamination in the unlabeled data. Particularly, our significantly improved precision-recall performance in unknown anomaly detection, *i.e.*, 10%-30%, is very encourage in that (i) it is already very challenging to improve this metric for known anomalies, and the challenge is further largely increased for the unknown anomalies; and (ii) detecting unknown anomalies is one of the most critical open problems and of tremendous interest in numerous real-world applications. Our results may suggest the labeled anomaly data, regardless of its scale, should be fully leveraged to enable more accurate and comprehensive anomaly detection.

The proposed technique may be further improved to consider, beyond pairwise, listwise relation. Pretraining our models with some relevant large-scale unlabeled data may help train deeper neural networks and further improve the detection performance. It is also subject to future research on whether the proposed technique could be extended to interpret the anomalies detected.

References

- Charu C Aggarwal. *Outlier analysis*. Springer, 2017.
- Charu C Aggarwal and Saket Sathe. Theoretical foundations and algorithms for outlier ensembles. *ACM Sigkdd Explorations Newsletter*, 17(1):24–47, 2015.
- Kendrick Boyd, Kevin H Eng, and C David Page. Area under the precision-recall curve: point estimates and confidence intervals. In *ECML/PKDD*, pages 451–466. Springer, 2013.
- Markus M Breunig, Hans-Peter Kriegel, Raymond T Ng, and Jörg Sander. LOF: Identifying density-based local outliers. In *ACM Sigmod Record*, volume 29, pages 93–104. ACM, 2000.
- Toon Calders and Szymon Jaroszewicz. Efficient auc optimization for classification. In *PKDD*, pages 42–53. Springer, 2007.
- Raghavendra Chalapathy, Aditya Krishna Menon, and Sanjay Chawla. Anomaly detection using one-class neural networks. *arXiv preprint arXiv:1802.06360*, 2018.
- Jinghui Chen, Saket Sathe, Charu Aggarwal, and Deepak Turaga. Outlier detection with autoencoder ensembles. In *SDM*, pages 90–98. SIAM, 2017.
- Corinna Cortes and Mehryar Mohri. Auc optimization vs. error rate minimization. In *NeurIPS*, pages 313–320, 2004.
- Elad Eban, Mariano Schain, Alan Mackey, Ariel Gordon, Ryan Rifkin, and Gal Elidan. Scalable learning of non-decomposable objectives. In *AISTATS*, pages 832–840, 2017.
- Charles Elkan and Keith Noto. Learning classifiers from only positive and unlabeled data. In *KDD*, pages 213–220. ACM, 2008.
- Li Fei-Fei, Rob Fergus, and Pietro Perona. One-shot learning of object categories. *IEEE Transactions on Pattern Analysis and Machine Intelligence*, 28(4):594–611, 2006.
- Alberto Fernández, Salvador García, Mikel Galar, Ronaldo C Prati, Bartosz Krawczyk, and Francisco Herrera. *Learning from imbalanced data sets*. Springer, 2018.
- Wei Gao and Zhi-Hua Zhou. On the consistency of auc pairwise optimization. In *IJCAI*, pages 939–945, 2015.
- Xavier Glorot and Yoshua Bengio. Understanding the difficulty of training deep feedforward neural networks. In *AISTATS*, pages 249–256, 2010.
- Ian Goodfellow, Yoshua Bengio, and Aaron Courville. *Deep learning*. MIT press, 2016.
- Nico Görmitz, Marius Kloft, Konrad Rieck, and Ulf Brefeld. Toward supervised anomaly detection. *Journal of Artificial Intelligence Research*, 46:235–262, 2013.
- Josif Grabocka, Randolph Scholz, and Lars Schmidt-Thieme. Learning surrogate losses. *arXiv preprint arXiv:1905.10108*, 2019.
- Simon Hawkins, Hongxing He, Graham Williams, and Rohan Baxter. Outlier detection using replicator neural networks. In *DaWaK*, 2002.
- Haibo He and Eduardo A Garcia. Learning from imbalanced data. *IEEE Transactions on knowledge and data engineering*, 21(9):1263–1284, 2009.
- Dino Ienco, Ruggero G Pensa, and Rosa Meo. A semisupervised approach to the detection and characterization of outliers in categorical data. *IEEE Transactions on Neural Networks and Learning Systems*, 28(5):1017–1029, 2017.
- Huidong Jin, Jie Chen, Hongxing He, Graham J Williams, Chris Kelman, and Christine M O’Keefe. Mining unexpected temporal associations: applications in detecting adverse drug reactions. *IEEE Transactions on Information Technology in Biomedicine*, 12(4):488–500, 2008.
- Huidong Jin, Jie Chen, Hongxing He, Chris Kelman, Damien McAullay, and Christine M O’Keefe. Signaling potential adverse drug reactions from administrative health databases. *IEEE Transactions on Knowledge and Data Engineering*, 22(6):839–853, 2010.
- Hans-Peter Kriegel, Matthias Schubert, and Arthur Zimek. Angle-based outlier detection in high-dimensional data. In *KDD*, pages 444–452. ACM, 2008.
- Xiaoli Li and Bing Liu. Learning to classify texts using positive and unlabeled data. In *IJCAI*, volume 3, pages 587–592, 2003.
- Fei Tony Liu, Kai Ming Ting, and Zhi-Hua Zhou. Isolation-based anomaly detection. *ACM Transactions on Knowledge Discovery from Data*, 6(1):3, 2012.
- Mary McGlohon, Stephen Bay, Markus G Anderle, David M Steier, and Christos Faloutsos. SNARE: A link analytic system for graph labeling and risk detection. In *KDD*, pages 1265–1274. ACM, 2009.
- Pritish Mohapatra, CV Jawahar, and M Pawan Kumar. Efficient optimization for average precision svm. In *NeurIPS*, pages 2312–2320, 2014.
- Nour Moustafa and Jill Slay. UNSW-NB15: a comprehensive data set for network intrusion detection systems. In *Military Communications and Information Systems Conference, 2015*, pages 1–6, 2015.

- Keith Noto, Carla Brodley, and Donna Slonim. FRaC: a feature-modeling approach for semi-supervised and unsupervised anomaly detection. *Data Mining and Knowledge Discovery*, 25(1):109–133, 2012.
- Guansong Pang, Longbing Cao, Ling Chen, and Huan Liu. Learning representations of ultrahigh-dimensional data for random distance-based outlier detection. In *KDD*, pages 2041–2050, 2018.
- Guansong Pang, Chunhua Shen, and Anton van den Hengel. Deep anomaly detection with deviation networks. In *KDD*, pages 353–362. ACM, 2019.
- Guansong Pang, Chunhua Shen, Longbing Cao, and Anton van den Hengel. Deep learning for anomaly detection: A review. *ACM Computing Surveys*, 2020. In press.
- Luis Perez and Jason Wang. The effectiveness of data augmentation in image classification using deep learning. *arXiv preprint:1712.04621*, 2017.
- Steffen Rendle, Christoph Freudenthaler, Zeno Gantner, and Lars Schmidt-Thieme. Bpr: Bayesian personalized ranking from implicit feedback. In *UAI*, pages 452–461, 2009.
- Lukas Ruff, Nico Görnitz, Lucas Deecke, Shoaib Ahmed Siddiqui, Robert Vandermeulen, Alexander Binder, Emmanuel Müller, and Marius Kloft. Deep one-class classification. In *ICML*, pages 4390–4399, 2018.
- Lukas Ruff, Robert A Vandermeulen, Nico Görnitz, Alexander Binder, Emmanuel Müller, Klaus-Robert Müller, and Marius Kloft. Deep semi-supervised anomaly detection. *arXiv preprint arXiv:1906.02694*, 2019.
- Emanuele Sansone, Francesco GB De Natale, and Zhi-Hua Zhou. Efficient training for positive unlabeled learning. *IEEE Transactions on Pattern Analysis and Machine Intelligence*, 2018.
- Thomas Schlegl, Philipp Seeböck, Sebastian M Waldstein, Ursula Schmidt-Erfurth, and Georg Langs. Un-supervised anomaly detection with generative adversarial networks to guide marker discovery. In *IPMI*, pages 146–157. Springer, Cham, 2017.
- Yiyuan She and Art B Owen. Outlier detection using nonconvex penalized regression. *Journal of the American Statistical Association*, 106(494):626–639, 2011.
- Jake Snell, Kevin Swersky, and Richard Zemel. Prototypical networks for few-shot learning. In *NeurIPS*, pages 4077–4087, 2017.
- Mahito Sugiyama and Karsten Borgwardt. Rapid distance-based outlier detection via sampling. In *NeurIPS*, pages 467–475, 2013.
- Acar Tamersoy, Kevin Roundy, and Duen Horng Chau. Guilt by association: Large scale malware detection by mining file-relation graphs. In *KDD*, pages 1524–1533, 2014.
- David MJ Tax and Robert PW Duin. Support vector data description. *Machine Learning*, 54(1):45–66, 2004.
- Vincent Vercruyssen, Wannes Meert, Gust Verbruggen, Koen Maes, Ruben Baumer, and Jesse Davis. Semi-supervised anomaly detection with an application to water analytics. In *ICDM*, volume 2018, pages 527–536. IEEE, 2018.
- Oriol Vinyals, Charles Blundell, Timothy Lillicrap, Daan Wierstra, et al. Matching networks for one shot learning. In *NIPS*, pages 3630–3638, 2016.
- RF Woolson. Wilcoxon signed-rank test. *Wiley Encyclopedia of Clinical Trials*, pages 1–3, 2007.
- Mingxi Wu and Christopher Jermaine. Outlier detection by sampling with accuracy guarantees. In *KDD*, pages 767–772, 2006.
- Chun Yu and Weixin Yao. Robust linear regression: A review and comparison. *Communications in Statistics-Simulation and Computation*, 46(8):6261–6282, 2017.
- Houssam Zenati, Manon Romain, Chuan-Sheng Foo, Bruno Lecouat, and Vijay Chandrasekhar. Adversarially learned anomaly detection. In *ICDM*, pages 727–736. IEEE, 2018.
- Ke Zhang, Marcus Hutter, and Huidong Jin. A new local distance-based outlier detection approach for scattered real-world data. In *PAKDD*, pages 813–822. Springer, 2009.
- Xiang Zhang and Yann LeCun. Text understanding from scratch. *arXiv preprint:1502.01710*, 2015.
- Ya-Lin Zhang, Longfei Li, Jun Zhou, Xiaolong Li, and Zhi-Hua Zhou. Anomaly detection with partially observed anomalies. In *WWW Companion*, pages 639–646, 2018.
- Panpan Zheng, Shuhan Yuan, Xintao Wu, Jun Li, and Aidong Lu. One-class adversarial nets for fraud detection. In *AAAI*, volume 33, pages 1286–1293, 2019.
- Zhi-Hua Zhou. A brief introduction to weakly supervised learning. *National Science Review*, 5(1):44–53, 2018.
- Arthur Zimek, Matthew Gaudet, Ricardo JGB Campello, and Jörg Sander. Subsampling for efficient and effective unsupervised outlier detection ensembles. In *KDD*, pages 428–436. ACM, 2013.
- Bo Zong, Qi Song, Martin Renqiang Min, Wei Cheng, Cristian Lumezanu, Daeki Cho, and Haifeng Chen. Deep autoencoding gaussian mixture model for unsupervised anomaly detection. In *ICLR*, 2018.